DESIGNING POROUS STRUCTURES FOR ORTHOPEDIC APPLICATIONS USING ADDITIVE MANUFACTURING

A Thesis

Presented to the Faculty of the Graduate School

of Cornell University

In Partial Fulfillment of the Requirements for the Degree of

Master of Science

by

Shonak Bhattacharya

May 2022

ABSTRACT

The need to develop better materials for fabricating orthopedic implants is the key to manufacturing longer lasting implants with a reduced chance of early failure and the need for revision surgeries. This work aims to provide a logical and methodical approach in designing porous structures using tools such as Topology Optimization (TO), Computer Aided Design (CAD) and Finite Element Analysis (FEA) alongside Additive Manufacturing (AM) to fabricate orthopedic implants.

Porous structures were designed using topology optimization to tailor mechanical properties that match that of the human bone. The mechanical properties of suitable structures were determined computationally using finite element analysis. Further, the structures depicting desirable properties were manufactured using Electron Beam Melting (EBM) to experimentally verify their mechanical properties.

The results show that we were able to successfully design a porous structure that had a Young's modulus as low as 1.7 GPa which falls well within the range of that of human bone making it a viable material for developing orthopedic implants.

BIOGRAPHICAL SKETCH

Shonak Bhattacharya received his Bachelor of Engineering from the University of Mumbai, India in 2019. After graduating, he joined Cornell University to pursue his Master's degree in Mechanical Engineering. In doing so, Shonak joined the Laboratory of Advanced Materials and Manufacturing (LAMM) to conduct research on using additive manufacturing techniques for biomedical applications.

To my mom, dad and sister for their constant love and support.

To my twin brother who always drives me to be the best version of myself.

And to true friends. May we all find a few.

More Life!

ACKNOWLEDGMENTS

I would like to thank my committee for guiding me throughout this research project. I would specially like to thank Professor Atieh Moridi, who in her capacity as my advisor guided me and mentored me to deliver this work to the best of my abilities. I would also like to extend my gratitude to Fernando Q. Gonzales from the Hospital of Special Surgery for helping me better understand the complexities surrounding this project and motivating me to achieve the best results.

TABLE OF CONTENTS

LIST OF FIGURES

LIST OF TABLES

CHAPTER ONE

INTRODUCTION AND BACKGROUND

1.1. Overview and Aims

The need for better materials for fabricating orthopedic implants is crucial for us to be able to manufacture longer lasting and mechanically superior implants. Doing so enables us to manufacture implants that have both, low risk for premature failure and lesser need for revision surgery which directly proves beneficial to the general population that use these medical devices. The aim of this thesis is to provide a logical and methodical approach to designing novel materials, or biomaterials, as they are used for biomedical purposes that are suitable substitutes for conventionally used biomaterials in order to fabricate such superior implants as suggested earlier. Using designing tools such as Topology Optimization (TO), Computer Aided Design (CAD) and Finite Element Analysis (FEA) and in complement to Additive Manufacturing (AM) it is possible to design and manufacture novel biomaterials that show non-conventional properties that are desired for orthopedic applications. A detailed approach on using these tools for the given purpose is discussed in Chapter 2. This chapter will provide a detailed conceptual understanding of the tools and concepts that are addressed in this work.

1.2. Conventional Implants and Their Drawbacks

1.2.1. Conventional Implants

Traditionally, metal orthopedic implants are manufactured using Titanium alloys, Cobalt Chromium Alloys or Stainless Steel. They are classified as two types:

permanent joint replacements, which are expected to remain in the body throughout the lifespan of the patient, and temporary orthopedic implants that serve for a short time as a healing aid for the bone[1].

1.2.2. Drawbacks

The human bone has a low Young's modulus (elastic modulus) that lies approximately between 3GPa and 18GPa[2]. In comparison to this, the conventional implants have a much higher value of elastic modulus (Fig 1.1).

This difference on elastic modulus between bone and implants may lead to the phenomena of stress-shielding. Stress-shielding is defined as the reduction of bone density caused by removal of typical stresses acting on a bone by the implant (Fig. 1.2)[3]. This is a result of Wolff's law which states that bone in a healthy human will remodel itself based on the loads it is placed under[4,5]. This phenomenon often leads to complications such as implant loosening, improper fixation and hindered biological functioning of the surrounding bone[6–8].

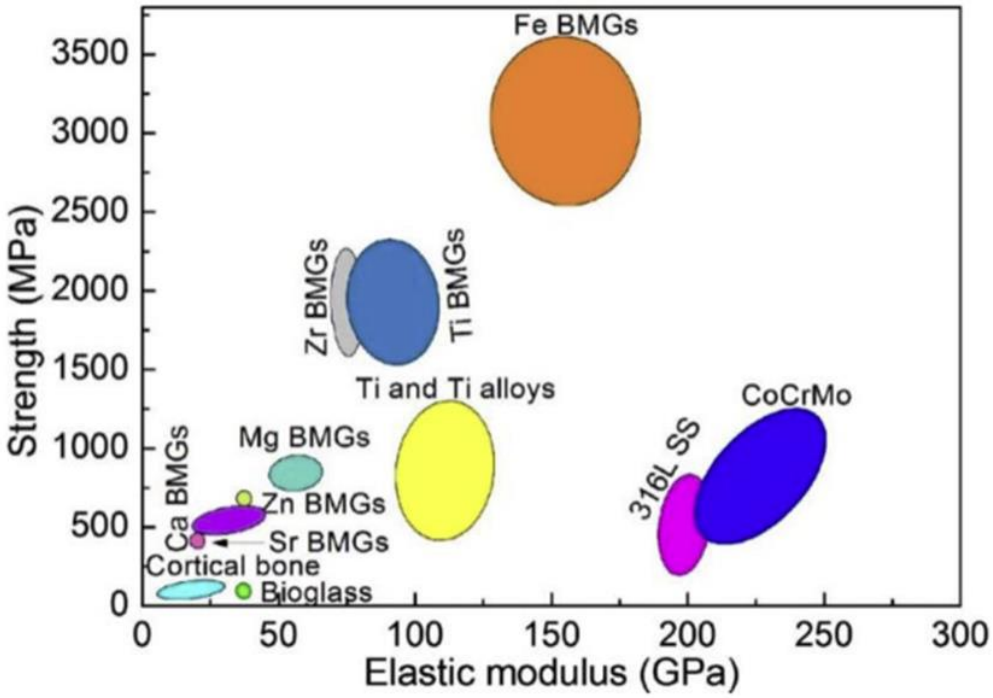

Figure 1.1. Strength v/s Elastic Modulus of Different Materials

Figure 1.2 Stress Shielding in a human bone

1.3. Topology Optimization

Topology Optimization (TO) is a mathematical approach that optimizes material layout within a given design space for a set of pre-defined boundary conditions such a load, boundaries, and constraints[9,10]. There are multiple approaches to a single problem and the commonly used algorithms are: (i) Solid Isotropic Material with Penalization (SIMP)[11]. (ii) Bi-directional Evolutionary Structural Optimization (BESO)[12] and (iii) Iso-Line Algorithm[13] (Fig. 1.3).

Using TO we can input the boundary conditions for a given application and see the outputs for structures that are suitable for it. Using this approach, we can compare multiple structures using tools like FEA (which will be explained in the next chapter) before

manufacturing them to determine which is the most suitable. This saves us the cost and time of manufacturing multiple structures and comparing them.

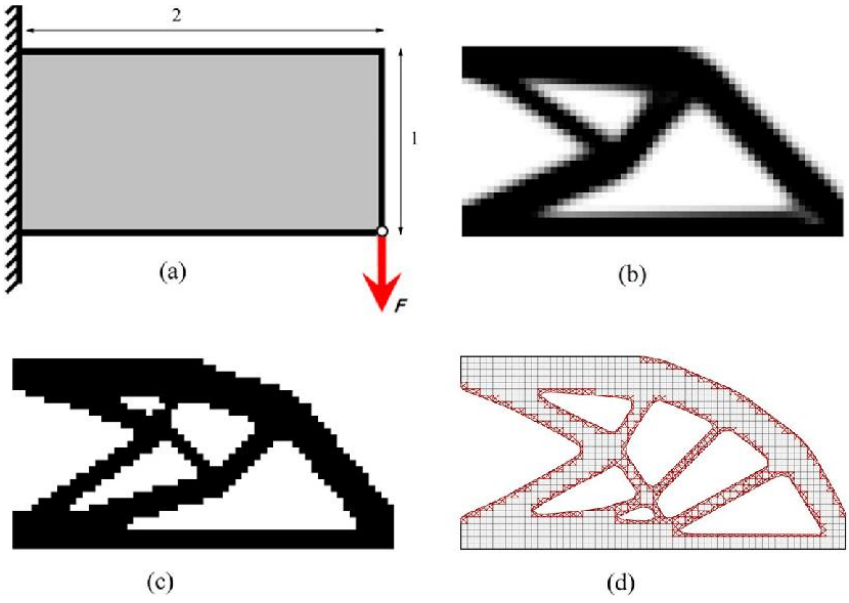

Figure 1.3 Different topology optimization algorithms (a) Boundary condition for a given application. (b) SIMP algorithm. (c) BESO algorithm (d) ISO line algorithm[14]

1.4. Finite Element Analysis

Finite Element Analysis (FEA) is a simulation technique used to predict how a part behaves under a set of given conditions. This prediction is done using a numeric method called Finite Element Method (FEM). This is a general numerical approach to solving partial differential equations in two or three boundary variables (space variables)[15]. To solve such a problem, FEM divides a large system into smaller parts called finite elements by space discretization. This is implemented by creation of a mesh of the object in consideration with a finite number of points. This formulation of a boundary problem results in a system of algebraic equations which is used to compute the unknown function over the given domain. These simple equations are then assembled into a larger system of equations that model the entire problem[16–18].

1.5. Additive Manufacturing

Additive Manufacturing (AM) or 3D printing involves the fabrication of three-dimensional objects directly from a CAD model. It involves a layer-by-layer process of fusing a feedstock (often powder or wire) together using a high energy source, in order to build the object from ground up, i.e., in an additive manner[19–21].

1.5.1. Processes and Types

There are multiple types of AM techniques such as Electron beam Melting, Selective Laser Melting, Selective Laser Sintering, Fuse Deposition Modelling, Direct Energy Deposition, to name a few. The most common methods of manufacturing parts for

biomedical applications however are Electron Beam Melting and Selective Laser Melting.

A) Electron Beam Melting

Electron Beam Melting (EBM) or Electron Beam Additive Manufacturing (EBAM) is a type of AM that utilizes a high energy electron beam as a moving heat source, to fuse metal powder to fabricate parts in a layer-by-layer fashion[22,23] (Fig. 1.4).

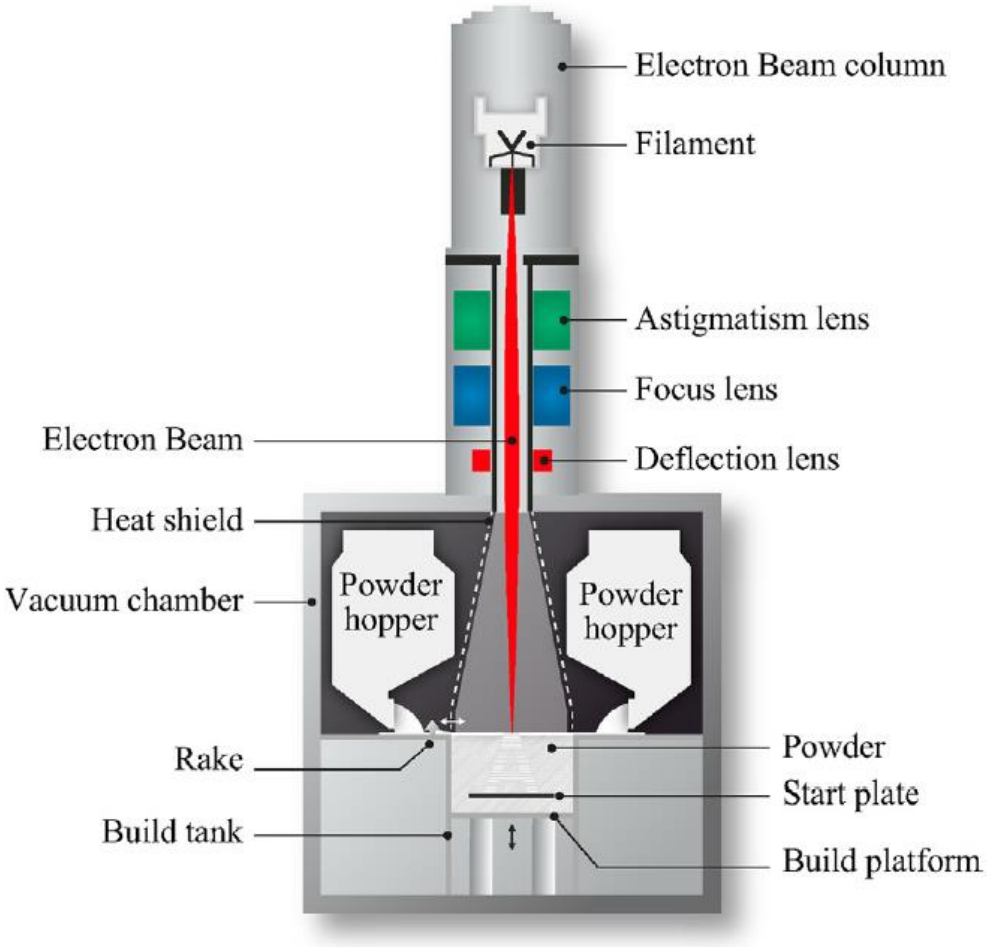

Figure 1.4 Schematic of an EBM Machine

B) Selective Laser Melting

Selective Laser Melting (SLM) or Direct Metal Laser Melting (DMLM) is 3D printing technique that uses a high-power density laser to fuse metallic powders together, once again in layer-by-layer fashion, to fabricate a part dictated by a CAD model[24–26] (Fig. 1.5).

1.5.2. Advantages

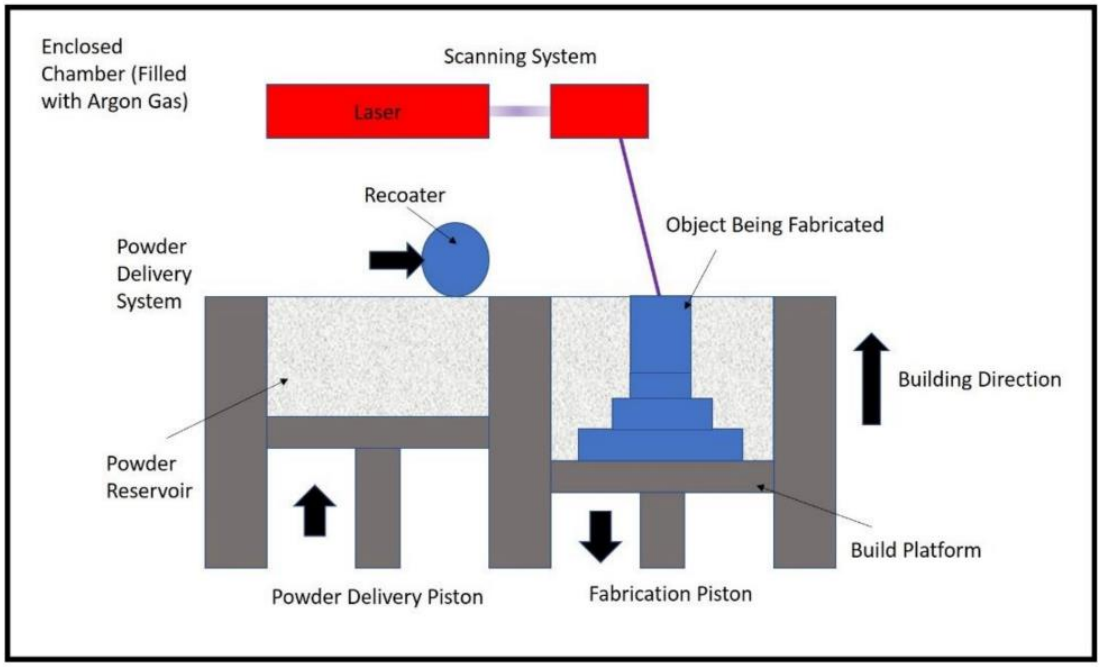

Figure 1.5 A schematic for an SLM Machine.

The layer-by-layer process of AM allows us to fabricate structures with complex geometries that cannot be manufactures using conventional manufacturing techniques. These complex structures can be tailored to show unnatural mechanical properties which can prove advantageous in various applications in aerospace, biomedical and thermal industries.

Moreover, the rapid prototyping ability of AM further allows for a faster path to fabricate complex parts for experimental testing as opposed taking the tedious route of conventional manufacturing techniques[27–30].

1.6. Biomedical Applications of Additive Manufacturing

The versatility and high resolution achieved by various AM techniques provides opportunities to engineer implants with hierarchical microstructures and tailored mechanical properties [31]. Furthermore, the implants can be made patient-specific and designed to achieve desired biomechanical responses to aid in the restoration of physiological functions, such as controlled displacements for respiratory expansion and contraction [32]. The current-state-of-the-art advances in biomedical applications are listed below [33].

1.6.1. Meta-Materials

The mechanical properties of conventional materials are primarily dictated by their chemical composition and their microstructure. Mechanical metamaterials challenge these conventional material definitions by engineering structures that exhibit counter-intuitive mechanical properties (e.g., materials that display remarkably low stiffness or a zero or negative Poisson's ratio). Metamaterials are often characterized by having ordered cellular lattices, such that their mechanical response and functionality relate to their density and can thus be controlled. In the fabrication of orthopaedic implants, metamaterials can provide structures with gradient porosities and stiffness similar to the intricate structure of bone in which cortical bone with high modulus (13.6GPa - 28GPa) morphs regionally into low modulus cancellous bone (0.02GPa - 0.64GPa) [32]. Complex metamaterial structures could serve to improve the interactions at the

bone-implant interface and also exhibit osteoconductive properties providing an optimized environment for tissue integration [27,34]. Meta-implants manufactured using tetrahedral unit cells and customized gradient densities have shown potential in reducing bone-loss resulting from stress shielding by ~75% [35].

Orthopaedic implants often incorporate intramedullary stems for fixation to the endosteal surfaces of long bones like the femur and humerus. The resulting implant bone composite is constantly subjected to bending and torsional loads, often leading to failure of the bone-implant interface. Moreover, debris (caused by fretting wear) can get trapped causing osteolysis [36]. The design of implants combining auxetic and non-auxetic metamaterials on the interfaces subject to tensile and compressive loading respectively, have shown the ability to eliminate the retraction of the implant from the bone by inducing expansion at both interfaces, even as the material undergoes tensile loading [37]. This can result in increased implant longevity and reduced need for revision surgery.

1.6.2. Patient-Specific Implants

Despite the widespread availability of implant systems with a number of sizes to fit a broad spectrum of anatomy, cases nonetheless arise in which a standard commercial device will not suffice. Examples include cases of dysplasia where the anatomy is grossly distorted or cases of revision surgery in which the failure of the original implant has led to significant bone loss. Developing solutions for such cases can be reached by the direct coupling of advanced imaging techniques, usually computed tomography (CT) and magnetic resonance imaging (MRI), and AM processes to engineer patient-specific implants. CT data has the added benefit of providing direct

high-resolution measurement of the density of the remaining bone. This information can be used to help design not just the shape of the implant, but it's local structural and mechanical properties. In this way load transfer between the implant and the surrounding remaining bone can be optimized to assure both short-term fixation and longevity [2,38]. The direct reconstruction of anatomical regions via CT images has been effectively implemented for the accurate design of orbital socket [39], hip [40] and sternal implants manufactured via AM techniques. The surgical procedures with sternal implants demonstrated immediate structural support and significant improvement in patients' respiratory symptoms postoperatively [41].

1.6.3. Absorbable Implants

Titanium alloys [6], cobalt-chromium alloys [42], tantalum, and stainless steel [43,44] are metallic materials commonly used in permanent orthopaedic implants due to their high structural integrity, corrosion resistance, and biocompatibility. However, numerous applications exist in which a lack of permanence is desired. For example, metallic plates and screws are often used to 'rigidly fix' fractured bones to facilitate healing. Once the fracture is healed, plates and screws can become a liability as a source of infection and stress shielding and at times can be a cause of discomfort for the patient. Moreover, in pediatric patients, metal implants must often be removed to allow bone growth as the child gets older. The process of removing the implant requires another surgery, which comes with an additional risk of surgical complications, pain and rehabilitation, and, of course, additional financial burden. Although, polymers have long been used to make resorbable implants, they do not meet the structural requirements needed in plates, screws, or most orthopaedic load

bearing implants. In addition, degradation of synthetic polymer-based resorbable structures can result in inflammation and the formation of ‘sterile’ abscesses [45]. Magnesium, iron and zinc are metals with bioresorbable properties and are essential trace metals in the human body [46]. Using alloys of these metals, implants can be manufactured with AM to have tuneable degradation rates that match the rate of bone formation for the given application reducing the risk of infection and cytotoxicity [47,48]. These implants could release metal ions that may be beneficial to the healing process [49].

The rapid growth of AM has equipped us with the capability to manufacture long-lasting implants with greater structural compatibility with the bone. AM processed implants have been effectively incorporated into surgical practice in recent years. The development of engineered metallic metamaterials with functional mechanical responses is a highly promising route to address some of the limitations of conventionally manufactured implants in terms of their geometry, density, strength, and stiffness. The application of CT imaging to reconstruct the affected region and fabricate patient-specific implants has resulted in unprecedented progress for reconstructive implants. Another benefit is the use of absorbable implants to provide temporary scaffolds to support bone healing without permanently remaining in the body.

Despite great progress in adopting AM for biomedical applications, certain areas require further improvement to develop the full potential of this disruptive manufacturing technology. Although the use of topology optimization is growing, we

are still far from mainstream adoption of this computational tool. In addition, improving metal AM resolution from microscale to nanoscale is required to advance the capability of printing complex structures. Improving geometrical fidelity could also result in greater implementation of topology optimization methods as we start to print smaller features with higher precision. However, an unsurmountable trade-off exists between deposition rate and accuracy that will remain a guiding limitation in the design of new processes with enhanced resolution. Similarly, the optimization of stiffness to enhance load sharing and load transfer between implant and bone cannot be done without consideration of fatigue, as orthopaedic implants are subjected to continual cyclic loading. This becomes a more complicated problem as we print materials with ever more complex geometries. Understanding the deformation mechanisms and the effects of feature size/length scale and interconnectivity on mechanical (and degradation) properties of implants is important to ensure proper implant design.

Scientific knowledge and engineering limitations are not the only factors currently hampering the widespread use of AM in orthopaedic devices. Necessary regulation by the FDA to ensure the safety and efficacy of orthopaedic implants is an important factor when adopting AM into manufacturing of both standard and patient-specific implants. Areas that must be considered as part of the regulation of AM manufactured implants include: the starting materials; design, printing, and post-printing validation of the AM process; printing characteristics and parameters; physical and mechanical assessment of the final implants; and biological considerations of these implants, including cleaning, sterility, and biocompatibility. The FDA has been working with

the commercial, clinical, and scientific communities to provide guidance on AM in medical devices [50].

1.7. Thesis Objectives

The aim of this thesis is to provide a methodical approach to designing porous structures for orthopedic applications. These structures are tailored to show a elastic modulus that matches or is close to that of bone in order to avoid complications that arise such as stress shielding. We used TO to design unit cells that could be used to fabricate porous lattice structures. These unit cells were then converted to CAD model and their mechanical properties were predicted using FEA. Following this, suitable structures were selected and printed using EBM for experimental verification of their mechanical properties. A structural analysis was also conducted keeping in mind the defects that arise from AM in order to justify any deviations in experimental results from computational predictions. Chapter 2 talks about the procedure followed in this work in detail.

REFERENCES

[1] W. Jin, P.K. Chu, Orthopedic Implants, in: R. Narayan (Ed.), Encycl. Biomed. Eng., Elsevier, Oxford, 2019: pp. 425–439. https://doi.org/https://doi.org/10.1016/B978-0-12-801238-3.10999-7.

[2] L. Zhang, L. Chen, A Review on Biomedical Titanium Alloys: Recent Progress and Prospect, Adv. Eng. Mater. 21 (2019) 1801215. https://doi.org/10.1002/adem.201801215.

[3] D.R. Sumner, Long-term implant fixation and stress-shielding in total hip replacement, J. Biomech. 48 (2015) 797–800. https://doi.org/10.1016/j.jbiomech.2014.12.021.

[4] S.C. Cowin, Wolff's law of trabecular architecture at remodeling equilibrium, J. Biomech. Eng. 108 (1986) 83–88. https://doi.org/10.1115/1.3138584.

[5] P.J. Prendergast, R. Huiskes, The Biomechanics of Wolff's law: Recent advances, Ir. J. Med. Sci. 164 (1995) 152–154. https://doi.org/10.1007/BF02973285.

[6] S.J. Macinnes, the Genetics of Osteolysis and Heterotopic Ossification After Total Hip Arthroplasty, (2016).

[7] M. Sundfeldt, L. V. Carlsson, C.B. Johansson, P. Thomsen, C. Gretzer, Aseptic loosening, not only a question of wear: A review of different theories, Acta Orthop. 77 (2006) 177–197. https://doi.org/10.1080/17453670610045902.

[8] R. Huiskes, H. Weinans, B. Van Rietbergen, The relationship between stress shielding and bone resorption around total hip stems and the effects of flexible

materials, Clin. Orthop. Relat. Res. (1992) 124–134. https://doi.org/10.1097/00003086-199201000-00014.

[9] P. Vogiatzis, S. Chen, X. Wang, T. Li, L. Wang, Topology optimization of multi-material negative Poisson's ratio metamaterials using a reconciled level set method, CAD Comput. Aided Des. 83 (2017) 15–32. https://doi.org/10.1016/j.cad.2016.09.009.

[10] V.J. Challis, J.K. Guest, Level set topology optimization of fluids in Stokes flow, Int. J. Numer. Methods Eng. 79 (2009) 1284–1308. https://doi.org/10.1002/nme.2616.

[11] D. Tcherniak, Topology optimization of resonating structures using SIMP method, Int. J. Numer. Methods Eng. 54 (2002) 1605–1622. https://doi.org/10.1002/nme.484.

[12] K. Ghabraie, An improved soft-kill BESO algorithm for optimal distribution of single or multiple material phases, Struct. Multidiscip. Optim. 52 (2015) 773–790. https://doi.org/10.1007/s00158-015-1268-2.

[13] K. Maute, E. Ramm, Adaptive topology optimization, Struct. Optim. 10 (1995) 100–112. https://doi.org/10.1007/BF01743537.

[14] M. Abdi, I. Ashcroft, R. Wildman, Topology optimization of geometrically nonlinear structures using an evolutionary optimization method, Eng. Optim. 50 (2018) 1850–1870. https://doi.org/10.1080/0305215X.2017.1418864.

[15] D.L. Logan, A First Course in the Finite Element Method, Cengage Learning, 2011. https://books.google.com/books?id=KGZtCgAAQBAJ.

[16] M. Yetmez, Finite element analysis, Musculoskelet. Res. Basic Sci. (2016) 51–

59. https://doi.org/10.1007/978-3-319-20777-3_4.

[17] K.-J. Bathe, Finite Element Method, in: Wiley Encycl. Comput. Sci. Eng., American Cancer Society, 2008: pp. 1–12. https://doi.org/https://doi.org/10.1002/9780470050118.ecse159.

[18] P. Kurowski, Finite Element Analysis for Design Engineers, in: Finite Elem. Anal. Des. Eng., 2017: pp. i–xiii.

[19] K. V. Wong, A. Hernandez, A Review of Additive Manufacturing, ISRN Mech. Eng. 2012 (2012) 1–10. https://doi.org/10.5402/2012/208760.

[20] W.E. Frazier, Metal additive manufacturing: A review, J. Mater. Eng. Perform. 23 (2014) 1917–1928. https://doi.org/10.1007/s11665-014-0958-z.

[21] D. Herzog, V. Seyda, E. Wycisk, C. Emmelmann, Additive manufacturing of metals, Acta Mater. 117 (2016) 371–392. https://doi.org/10.1016/j.actamat.2016.07.019.

[22] L.E. Murr, S.M. Gaytan, D.A. Ramirez, E. Martinez, J. Hernandez, K.N. Amato, P.W. Shindo, F.R. Medina, R.B. Wicker, Metal Fabrication by Additive Manufacturing Using Laser and Electron Beam Melting Technologies, J. Mater. Sci. Technol. 28 (2012) 1–14. https://doi.org/10.1016/S1005-0302(12)60016-4.

[23] M. Galati, L. Iuliano, A literature review of powder-based electron beam melting focusing on numerical simulations, Addit. Manuf. 19 (2018) 1–20. https://doi.org/10.1016/j.addma.2017.11.001.

[24] E. Louvis, P. Fox, C.J. Sutcliffe, Selective laser melting of aluminium components, J. Mater. Process. Technol. 211 (2011) 275–284. https://doi.org/10.1016/j.jmatprotec.2010.09.019.

[25] L.C. Zhang, H. Attar, Selective Laser Melting of Titanium Alloys and Titanium Matrix Composites for Biomedical Applications: A Review, Adv. Eng. Mater. 18 (2016) 463–475. https://doi.org/10.1002/adem.201500419.

[26] C.Y. Yap, C.K. Chua, Z.L. Dong, Z.H. Liu, D.Q. Zhang, L.E. Loh, S.L. Sing, Review of selective laser melting: Materials and applications, Appl. Phys. Rev. 2 (2015) 41101. https://doi.org/10.1063/1.4935926.

[27] H. Kang, J.P. Long, G.D. Urbiel Goldner, S.A. Goldstein, S.J. Hollister, A paradigm for the development and evaluation of novel implant topologies for bone fixation: Implant design and fabrication, J. Biomech. 45 (2012) 2241–2247. https://doi.org/10.1016/j.jbiomech.2012.06.011.

[28] Y. Yang, G. Wang, H. Liang, C. Gao, S. Peng, L. Shen, C. Shuai, Additive manufacturing of bone scaffolds, Int. J. Bioprinting. 5 (2019) 1–25. https://doi.org/10.18063/IJB.v5i1.148.

[29] C.Y. Lin, N. Kikuchi, S.J. Hollister, A novel method for biomaterial scaffold internal architecture design to match bone elastic properties with desired porosity, J. Biomech. 37 (2004) 623–636. https://doi.org/10.1016/j.jbiomech.2003.09.029.

[30] T. Winkler, F.A. Sass, G.N. Duda, K. Schmidt-Bleek, A review of biomaterials in bone defect healing, remaining shortcomings and future opportunities for bone tissue engineering: The unsolved challenge, Bone Jt. Res. 7 (2018) 232–243. https://doi.org/10.1302/2046-3758.73.BJR-2017-0270.R1.

[31] P.H. Warnke, T. Douglas, P. Wollny, E. Sherry, M. Steiner, S. Galonska, S.T. Becker, I.N. Springer, J. Wiltfang, S. Sivananthan, Rapid prototyping: Porous

titanium alloy scaffolds produced by selective laser melting for bone tissue engineering, Tissue Eng. - Part C Methods. 15 (2009) 115–124. https://doi.org/10.1089/ten.tec.2008.0288.

[32] J. Moradiellos, S. Amor, G. Rocco, M. Vidal, A. Es Varela, Functional Chest Wall Reconstruction With a Biomechanical Three-Dimensionally Printed Implant, Ann Thorac Surg. 103 (2017) 389–91. https://doi.org/10.1016/10.1016/j.athoracsur.

[33] S. Bhattacharya, J. Bustillos, F.J. Quevedo González, J.A. Spector, A. Moridi, Biomedical Applications of Metal Additive Manufacturing: Current State-of-the-Art and Future Perspective, Am. J. Biomed. Sci. Res. 7 (2020) 6–10. https://doi.org/10.34297/ajbsr.2020.07.001103.

[34] P. Heinl, L. Müller, C. Körner, R.F. Singer, F.A. Müller, Cellular Ti-6Al-4V structures with interconnected macro porosity for bone implants fabricated by selective electron beam melting, Acta Biomater. 4 (2008) 1536–1544. https://doi.org/10.1016/j.actbio.2008.03.013.

[35] S.J. Hollister, Porous scaffold design for tissue engineering, Nat. Mater. 4 (2005) 518–524. https://doi.org/10.1038/nmat1421.

[36] J. Hyun, S. Wang, S. Yang, Topology optimization of the shear thinning non-Newtonian fluidic systems for minimizing wall shear stress, Comput. Math. with Appl. 67 (2014) 1154–1170. https://doi.org/10.1016/j.camwa.2013.12.013.

[37] L. Jiang, S. Chen, C. Sadasivan, X. Jiao, Structural topology optimization for generative design of personalized aneurysm implants: Design, additive manufacturing, and experimental validation, 2017 IEEE Healthc. Innov. Point

Care Technol. HI-POCT 2017. 2017-Decem (2017) 9–13. https://doi.org/10.1109/HIC.2017.8227572.

[38] V.J. Challis, A.P. Roberts, J.F. Grotowski, L.-C. Zhang, T.B. Sercombe, Prototypes for Bone Implant Scaffolds Designed via Topology Optimization and Manufactured by Solid Freeform Fabrication, Adv. Eng. Mater. 12 (2010) 1106–1110. https://doi.org/10.1002/adem.201000154.

[39] T.A. Schaedler, A.J. Jacobsen, A. Torrents, A.E. Sorensen, J. Lian, J.R. Greer, L. Valdevit, W.B. Carter, Ultralight metallic microlattices, Science (80-.). 334 (2011) 962–965. https://doi.org/10.1126/science.1211649.

[40] S. Arabnejad, B. Johnston, M. Tanzer, D. Pasini, Fully porous 3D printed titanium femoral stem to reduce stress-shielding following total hip arthroplasty, J. Orthop. Res. 35 (2017) 1774–1783. https://doi.org/10.1002/jor.23445.

[41] M.K. Kamel, A. Cheng, B. Vaughan, B. Stiles, Sternal Reconstruction Using Customized 3D-Printed Titanium Implants, Ann. Thorac. Surg. (2019). https://doi.org/10.1016/j.athoracsur.2019.09.087.

[42] H.M.A. Kolken, S. Janbaz, S.M.A. Leeflang, K. Lietaert, H.H. Weinans, A.A. Zadpoor, Rationally designed meta-implants: A combination of auxetic and conventional meta-biomaterials, Mater. Horizons. 5 (2018) 28–35. https://doi.org/10.1039/c7mh00699c.

[43] C. Celenk, P. Celenk, Bone Density Measurement Using Computed Tomography, Comput. Tomogr. - Clin. Appl. (2012). https://doi.org/10.5772/22884.

[44] V. Bruno, C. Berti, C. Barausse, M. Badino, R. Gasparro, D.R. Ippolito, P. Felice, Clinical Relevance of Bone Density Values from CT Related to Dental Implant Stability: A Retrospective Study, Biomed Res. Int. 2018 (2018). https://doi.org/10.1155/2018/6758245.

[45] P. Stoor, A. Suomalainen, C. Lindqvist, K. Mesimäki, D. Danielsson, A. Westermark, R.K. Kontio, Rapid prototyped patient specific implants for reconstruction of orbital wall defects, J. Cranio-Maxillofacial Surg. 42 (2014) 1644–1649. https://doi.org/10.1016/j.jcms.2014.05.006.

[46] Y. Jun, K. Choi, Design of patient-specific hip implants based on the 3D geometry of the human femur, Adv. Eng. Softw. 41 (2010) 537–547. https://doi.org/10.1016/j.advengsoft.2009.10.016.

[47] Y.L. Hao, S.J. Li, R. Yang, Biomedical titanium alloys and their additive manufacturing, Rare Met. 35 (2016) 661–671. https://doi.org/10.1007/s12598-016-0793-5.

[48] S. Limmahakhun, A. Oloyede, K. Sitthiseripratip, Y. Xiao, C. Yan, Stiffness and strength tailoring of cobalt chromium graded cellular structures for stress-shielding reduction, Mater. Des. 114 (2017) 633–641. https://doi.org/10.1016/j.matdes.2016.11.090.

[49] P.F. Santos, M. Niinomi, H. Liu, K. Cho, M. Nakai, Y. Itoh, T. Narushima, M. Ikeda, Fabrication of low-cost beta-type Ti-Mn alloys for biomedical applications by metal injection molding process and their mechanical properties, J. Mech. Behav. Biomed. Mater. 59 (2016) 497–507. https://doi.org/10.1016/j.jmbbm.2016.02.035.

[50] E. Karamian, M.R. Kalantar Motamedi, A. Khandan, P. Soltani, S. Maghsoudi, An in vitro evaluation of novel NHA/zircon plasma coating on 316L stainless steel dental implant, Prog. Nat. Sci. Mater. Int. 24 (2014) 150–156. https://doi.org/10.1016/j.pnsc.2014.04.001.

CHAPTER TWO

DESIGN AND EVALUATION OF POROUS MATERIALS FOR ORTHOPEDIC APPLICATIONS

2.1. Introduction

The last decade has seen leaps in the advancement of metal Additive Manufacturing (AM) technologies which has enabled it to be a promising asset in terms of innovative design and manufacturing of structures for a multitude of applications [1–3]. Metal AM typically involves a high energy source (electron beam, plasma, laser) that is used to cause fusion of a metallic feedstock (powder, wire, sheets) in a layer-by-layer fashion to generate structures that are defined by computer aided designs (CAD) [1,4]. This intrinsic layer-by-layer process of AM enables the fabrication of structures with complex geometries that conventional manufacturing methods cannot produce easily, if at all [3]. This added dimension of customization and higher levels of structural complexity of AM presents new solutions to multiple challenges in mechanical and material engineering.

AM can be used to manufacture complex lattice structures that have mechanical properties that are not found naturally, i.e., they have properties that are unachievable by the parent material (e.g. low Young's modulus, negative Poisson ratio) [5–8]. A lattice structure is ideally defined as topologically ordered, open-celled, three-dimensional structure, consisting of one or more repeating unit cells [9]. These structures can be tuned by the designer by altering various parameters such as their cell topology, strut diameter and cell size to exhibit desirable properties. As a result, these porous structures have received plenty of attention in the past few years. They

find application in a wide range of fields such as aerospace, acoustics, and more prominently biomedical engineering [10–16].

The predominant challenge in biomedical engineering is the inability of conventional orthopedic implants to mimic the mechanical properties of bone. The Young's modulus of prominent materials is a lot higher that of bone (1-18 GPa) [17]. For example, Ti-6Al-4V, the most popular parent material in orthopedics, has a Young's modulus of about 114 GPA which is a lot higher than that of bone. Other popular alloys such as Cobalt-Chromium alloys (210-250 GPa) and Stainless Steel (190 GPa) show significantly higher moduli as well. This leads to various complications such as improper fixation, loosening of the implant and hindered biological functions of the surrounding bone [18,19]. Often, these shortcomings are caused by *stress shielding* [20]. Stress-shielding is defined as the reduction in bone density caused by removal of typical stresses by an implant; the underlying principle of which is Wolff's law which states that bone in a healthy living being (animal or human) will remodel depending on the loads acting on it [20]. The high resolution and versatility achieved by AM provide opportunities to engineer orthopedic implants using lattice structures that have tailored mechanical properties based on the anatomical region of application [14,15,21,22]. In addition to this, since AM structures are dependent on a CAD model, patient-specific implants can be engineered using magnetic resonance imaging (MRI) and computed tomography (CT) [23–26]. This serves extremely useful in cases with dysplasia or cases where implant failure has caused significant bone loss and revision surgery is required. In the past, Electron Beam Melting (EBM) [27] and Selective Laser Melting (SLM) [28] have been used to fabricate cranio-facial [29], dental, finger

[30], hip [13,31], knee [32], and thoracic implants [33] with several devices having received United States Food and Drug Administration (FDA) clearance [33].

The study presented in this paper aims to provide a logical and methodical approach to designing porous structures for biomedical applications using tools such as Topology Optimization [34,35], CAD, Finite Element Analysis (FEA) that complement AM well. Using topology optimization, unit cells were designed that would be best suited for applications where uniaxial loading was predominant followed by conversion to lattice structures by repeating these unit cells in a 3-dimensional array [36,37]. FEA was then used to computationally calculate the mechanical properties of these structures to determine if they lie in the target design space (viz. similarities to properties of bone). Properties under static and cyclic loading were calculated. Suitable structures were selected for printing and experimental verification of computationally calculated mechanical properties.

2.2. MATERIALS AND METHODS

2.2.1. Materials

Titanium alloy, Ti6Al4V (Ti64) was selected as the parent material for the structures discussed in this paper. This is because of its high strength, high corrosion resistance and great biocompatibility, which makes it the supreme choice for manufacturing orthopedic implants [38]. In addition to having a Young's modulus lower than other conventionally used parent materials in orthopedics, AM Ti64 structures have been reported to outperform their conventionally manufactured counterparts [39]. However, mechanical properties of Ti64 scaffolds, as with most scaffolds, are usually lower than in theory due to certain manufacturing constraints which cause deviations

from ideal structures [40,41]. Thus, it is important to account for this during the design phase by considering higher loads and incorporating a factor of safety.

2.2.2. Post Retrieval Analysis

To better understand the interactions between the implant and bone, an analysis of a failed tibial base plate retrieved from a patient (Fig. 2.1. A). was conducted. It can be clearly seen that some areas have bone still stuck to the surface while other regions do not. On viewing under a Scanning Electron Microscope (SEM) it can be observed that bone in fact has grown into the irregularities in certain regions (Fig. 2.1 B) whereas it is absent from other regions (Fig. 2.1 C). This could be because the bone failed to grow into the pores in the first place or that the bone resorbed in those regions.

This further adds to the advantage of having porous structures for fabricating implants as bone growing into the pores will not only provide better interlocking but also provide structural integrity to the implant structure by acting as a reinforcement [41].

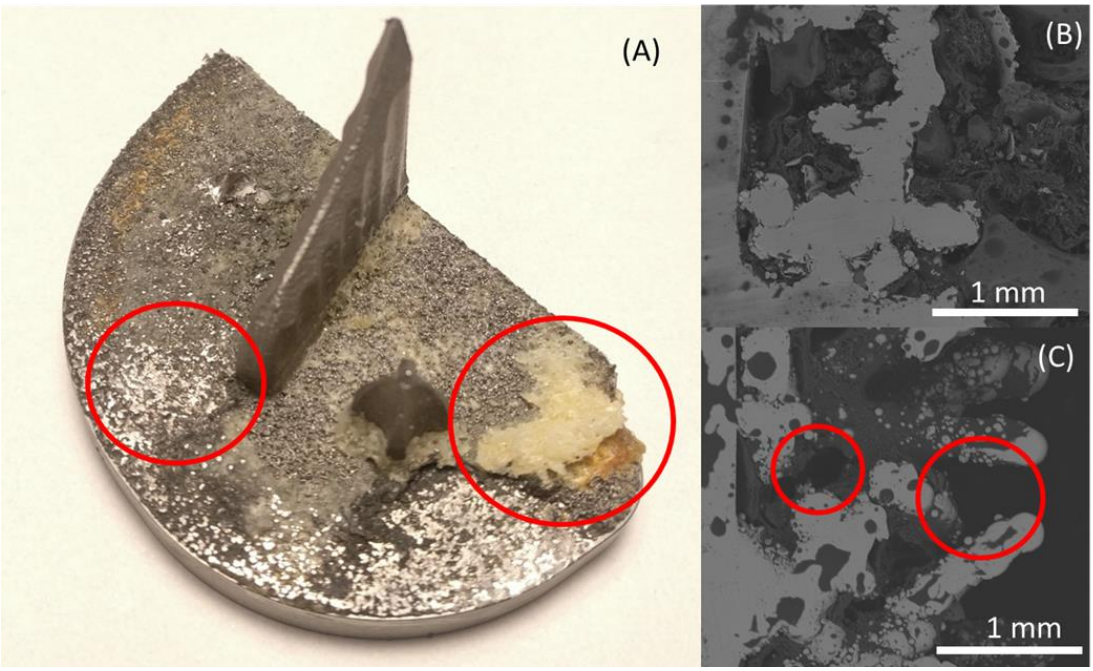

Figure 2.1 (A) Retrieved Tibial Base Plate showing regions with and without bone. (B) Bone ingrowth is seen in the irregularities. (C) Bone is absent in irregularities in other regions.

2.2.3. Design of Topologically Optimized Structures

The unit cell for the lattice structure was obtained using a topology optimization code that is based on the SIMP algorithm [37,42]. A uniaxial loading condition was used, and appropriate unit cells were chosen, i.e., ones that were porous and repeatable in a three-dimensional array. To save computational cost, semi-unit cells were designed and mirrored about the mid-plane to create the entire unit cell and converted to a corresponding CAD model using Solidworks (Fig. 2.2). The 2 suitable unit cells were designed for 3 levels of porosity – 30%, 50% and 70%. The lattice structure comprised of a 10x10x10 array of these unit cells.

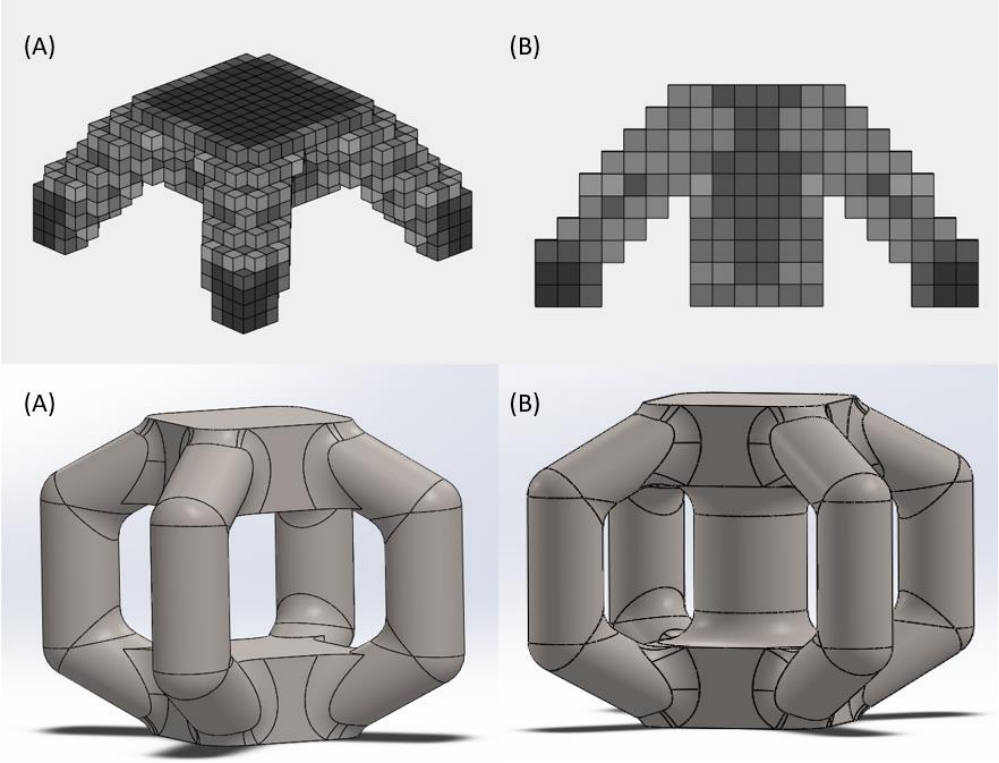

Figure 2.2 Shows the unit cells designed using topology optimization. (A) The topology optimized structure for Design 1 and it's corresponding CAD counterpart. (B) The topology optimized structure for Design 2 and it's corresponding CAD counterpart.

In addition to these topologically optimized structures, we designed a third structure by fortifying Design 1 with horizontal struts. This was done due to the suggestion that bone inspired lateral members could help improve the strength of such lattice structures [43]. Fig. 2.3 shows the unit cell for Design 3 with such horizontal struts.

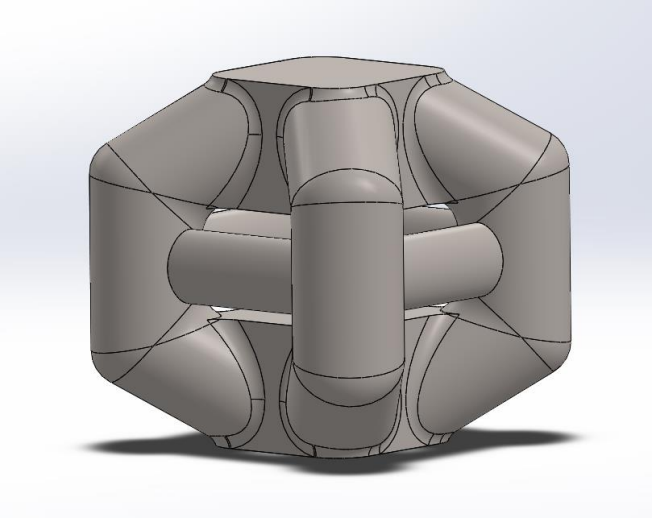

Figure 2.3 CAD model for the unit cell for Design 3

2.2.4. Computational Analysis

FEA software ANSYS was used to perform simulations on the 2 lattice structures and results were compared to standard unit cells – cube (high stiffness) and octahedron (relatively low stiffness) [44]. The unit cell geometry used in simulations was a 5x5x5 array of the unit cells, which is one-eight of the actual structure, with symmetric boundary conditions in order to save computational time [45]. Tests were performed under both static and cyclic loading with the goal of determining if the newly designed lattice structures showed suitable properties. This type of verification saves the cost of printing structures that do not show suitable properties in addition to providing an avenue to study expected behaviour. The material data used for the simulations was equivalent to Ti64 alloy and had the following properties – Young's modulus (E) = 114 GPa, Poisson ratio (ν) = 0.3 and density (ρ) = 4500 kg/m^3.

Static Loading Simulations

The loading force was determined using Bergmann's data and was calculated to be a maximum of 5kN [46,47]. The goal of these simulations was to calculate the apparent Young's modulus (E^*) of the structures to compare with that of bone and determine if they were suitable biomaterials. This modulus can be calculated using Eq. 1.

$$\boldsymbol{E^* = \frac{F}{A} \times \frac{l}{\Delta l}} \quad \textbf{MPa} \tag{1}$$

Where, F = compressive force (N), A = Area of cross-section including pores (mm^2), l = length of the structure in the direction of loading (mm) and Δl = change in the length of specimen in the direction of loading (mm).

Cyclic Loading Simulations

Compression-compression fatigue simulations were carried out on the 4 lattice structures considered in this paper. The goal was to determine the fatigue limit of these structures and more specifically to determine if the unit cells could last a million cycles. This number of cycles is accepted as the benchmark in design of tibial implants as it corresponds to the number of steps a patient would take during the healing period [48]. Loads of 15 MPa (the operating load) and above were applied for the simulations.

2.2.5. Equipment and Manufacturing

Lattice structures which showed suitable properties in the computational simulations were chosen for printing and experimental verification. Structures were manufactured using the Arcam Q10 EBM machine often used for rapid prototyping. The machine

has a maximum beam power of 3000 W and a minimum beam diameter of 100 µm. The input to the printer is via an STL format of the CAD files. The maximum build size is 200x200x180mm and Ti64 powder was used as the material input. The structures were printed at a 45º angle to minimize supports. The as-printed structures are shown in Fig. 2.4.

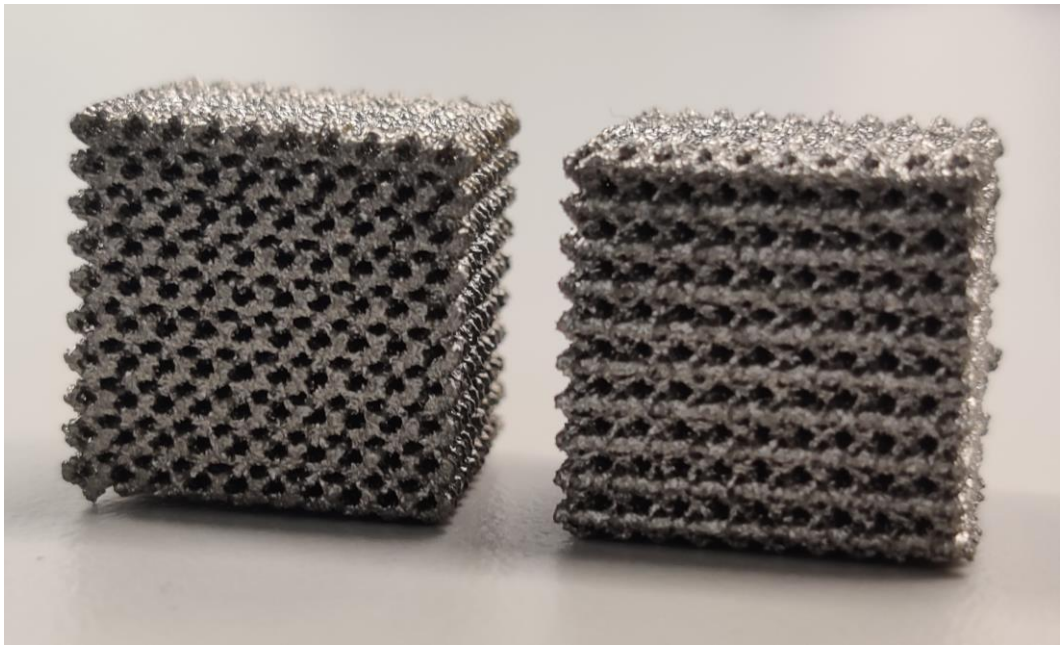

Figure 2.4 The as-printed structures. Design 1 is on the left and Octahedron is on the right.

2.2.6. Structural Characterization

External characterization of the printed structures was conducted under an SEM to study the surface characteristics and pore morphology [49]. Due to the nature of these lattices, printed structures often deviate from the ideal structure resulting in lower mechanical properties when compared to computational results.

2.2.7. Mechanical Testing

The mechanical behaviour of porous titanium is dependent on the porosity of the part. The effective stiffness and mechanical strength will reduce as the porosity increases

[50,51]. A simple axial compression test was performed on the printed samples to evaluate the Young's modulus. The maximum load of the machine was 100 kN and tests were performed at a crosshead speed of 1.8 mm/min [44]. Stress-strain curves were generated for each sample set.

2.3. Results

2.3.1. Computational Analysis

A) Static Properties

The Young's modulus was calculated for the 4 lattice structures. It is observed that as the porosity increases, the stiffness decreases. As the amount of material reduces with an increasing porosity, this directly corresponds to a weaker structure because the metal material is the only support material. Fig. 2.5. Shows the relation between the compressive Young's modulus and porosity. It can be clearly seen that Design 1 has the lowest modulus out of all the structures which is also within the range of that of bone. On the other hand, Design 2 showed the highest modulus, even higher than cube which is considered the stiffest conventional unit cell.

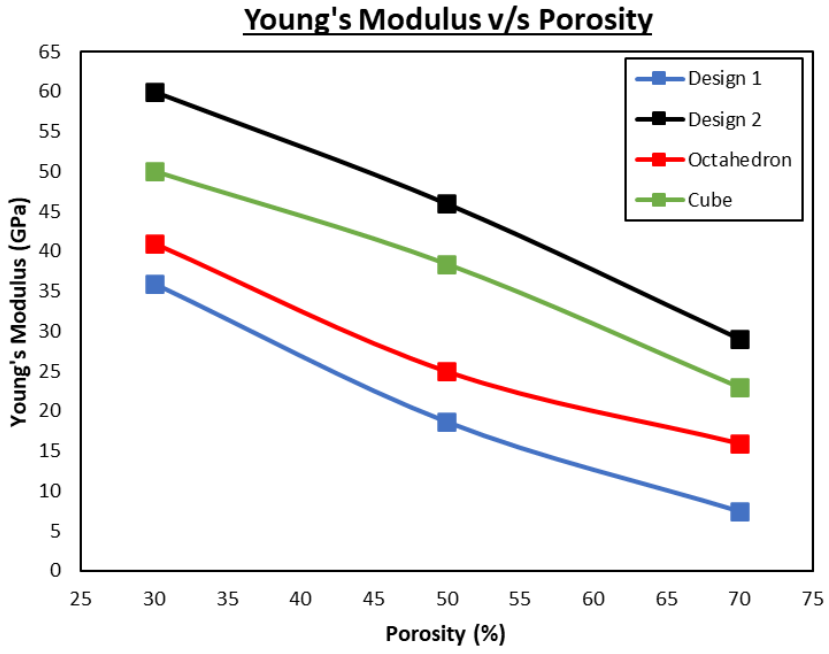

Figure 2.5 Graph depicting the Young's modulus V. Porosity for the 4 structures.

Fig 2.6 shows how the 4 lattice structures bear stress. Compression was simulated at 35 MPa which is higher than the application load for the given purpose. As seen, Design 1 and Octahedron develop similar maximum stress whereas Design 2 and Cube develop similar max stresses. As expected, the stress concentrations are present at joints Design 1 and the octahedron due to angular struts. Cube and Design 3 bear most of the stresses in the vertical members and hence have a higher stiffness than their counterparts. It is important to note that the maximum stress developed in the high stiffness structures is significantly higher than the low stiffness structures as seen in the figure below.

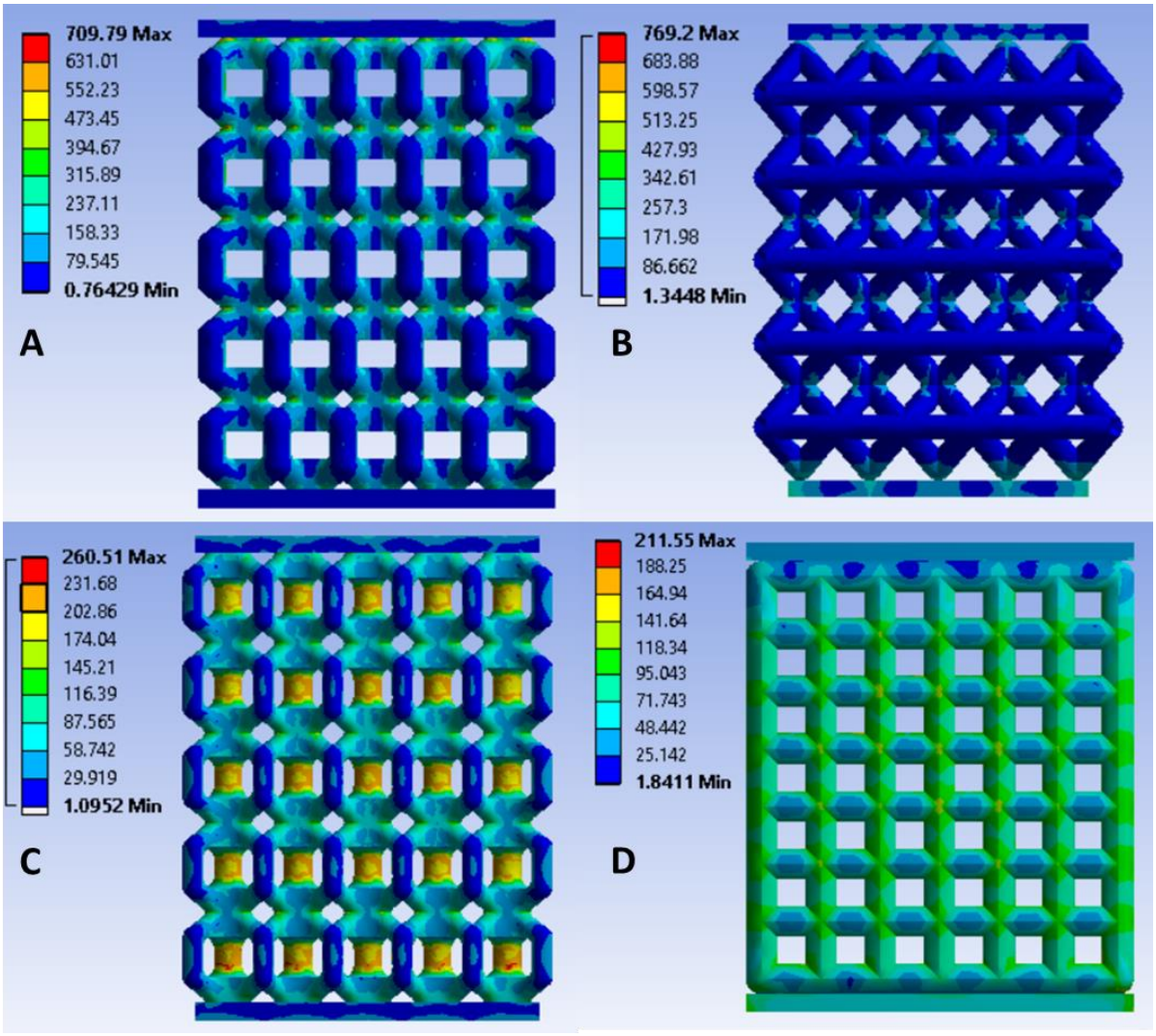

Figure 2.6. Stress concentrations developed on all 4 lattice structures. A. Design 1. B. Octahedron. C. Design 2. D. Cube.

B) Fatigue Properties

Fig. 2.7. shows the relation between the fatigue strength and porosity. As with the static properties, an inverse relation is observed between the fatigue strength and the porosity. Here the lattice structures clearly for two groups – the structures with higher

stiffness (design 2 and cube) show high fatigue strengths whereas the low stiffness structures (design 1 and octahedron) have lower fatigue strengths.

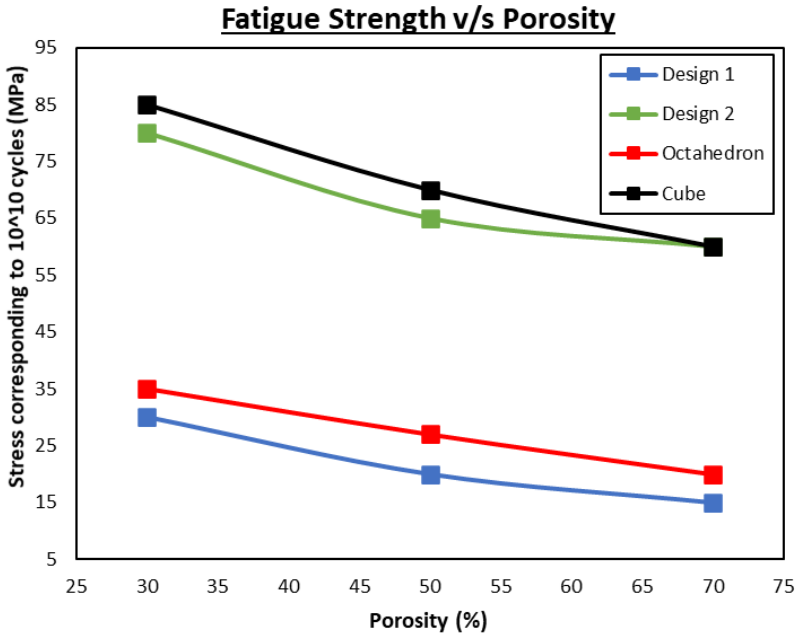

Figure 2.7. Graph of the Fatigue Strength corresponding to 10^10 cycles v. Porosity.

As observed from these simulations, one can see that a conventional trade-off exists between the elastic modulus and fatigue life. This often poses a problem when designing biomaterials because the goal is to get a very low modulus of elasticity and a sufficiently high fatigue life (Fig. 2.8.). illustrates this trade-off and highlights the region on the graph that is suitable for biomaterials. On plotting the Fatigue life v/s the Young's modulus for the 4 structures in the paper, only Design 1 falls in the suitable design space (Fig. 2.9.). The mechanical properties are summarized in Table 2.1.

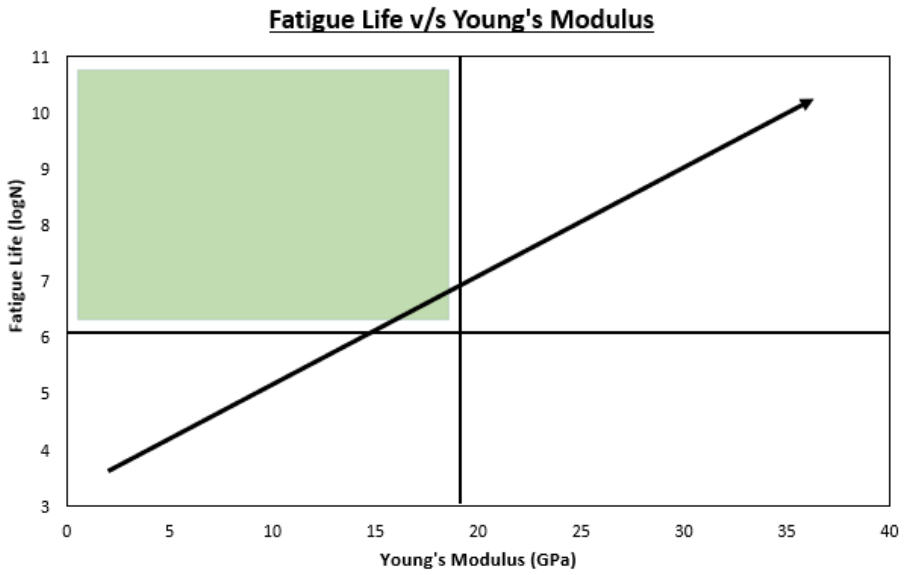

Figure 2.8. Showing the optimal design space for biomaterials used for orthopedic implants.

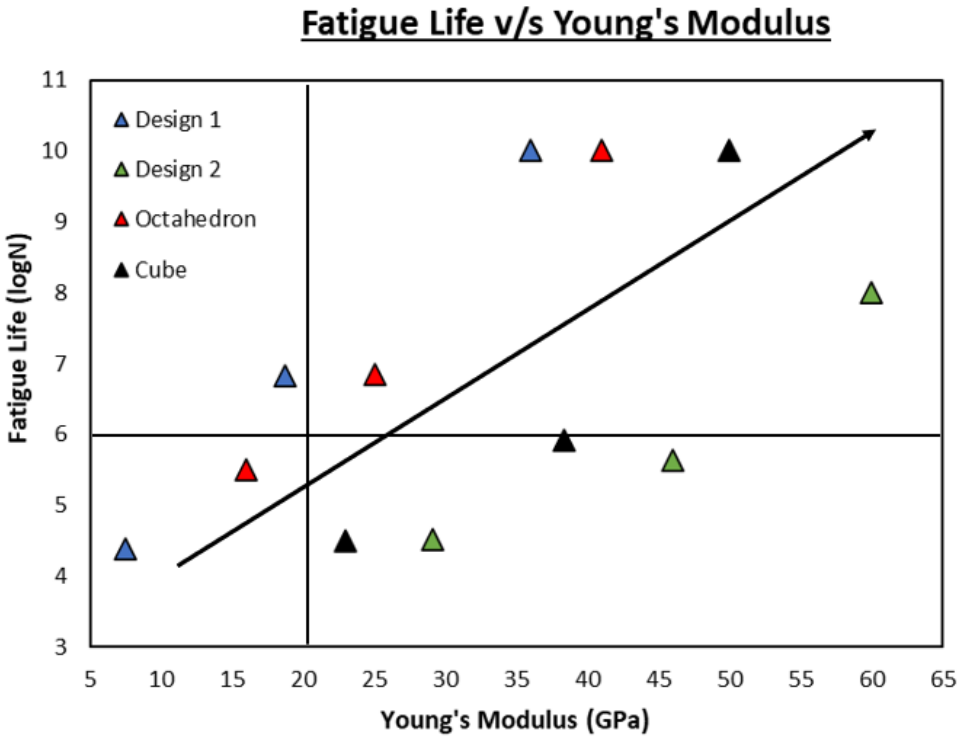

Figure 2.9. The Fatigue Life v. Young's Modulus for the 4 lattice structures.

Table 2.1: Shows the 4 lattice structures and their corresponding computational mechanical properties.

Unit Cell Type	Porosity	E (GPa)	Applied Stress (MPa)	Fatigue Life
Design 1	0.7	7.5	<15	$>10^6$
	0.5	18.7	<25	
	0.3	36	<30	
Design 2	0.7	29.1	<65	$>10^6$
	0.5	46	<70	
	0.3	60	<85	
Cube	0.7	23	<70	$>10^6$
	0.5	38.4	<85	
	0.3	50	<160	
Octahedron	0.7	18	<20	$>10^6$
	0.5	25	<25	
	0.3	41	<30	

Design 3, as introduced in *2.2.3*, was tested computationally to compare its behaviour with Design 1, which is the most suitable structure for our application (as seen in

Table 2.1 and Fig. 2.9). The mechanical properties of Design 3 in comparison to design 1 are highlighted in table 2.2.

Table 2.2: Shows the comparison between Design 1 and Design 3.

Unit Cell Type	Porosity (%)	Young's Modulus	Applied Stress	Fatigue Life
Design 1	70	7.5	<15	$>10^6$
	50	18.7	<25	
	30	36	<30	
Design 3	70	8.1	<10	$>10^6$
	50	19.5	<15	
	30	37.5	<20	

As seen, the addition of horizontal struts does not improve the behaviour of the lattice structure. In fact, in our case, design 1 performed better than design 3 in all aspects by showing a lower Young's modulus at all porosities and having a better fatigue strength.

For sake of comparison - A 30% porous structure of Design 3 showed similar induced yield stress to a 50% Design 1 structure (Fig. 2.10). This potentially could be a result of the added regions of stress concentrations arising from the joints of the horizontal struts and the vertical members as seen in Fig. 2.11.

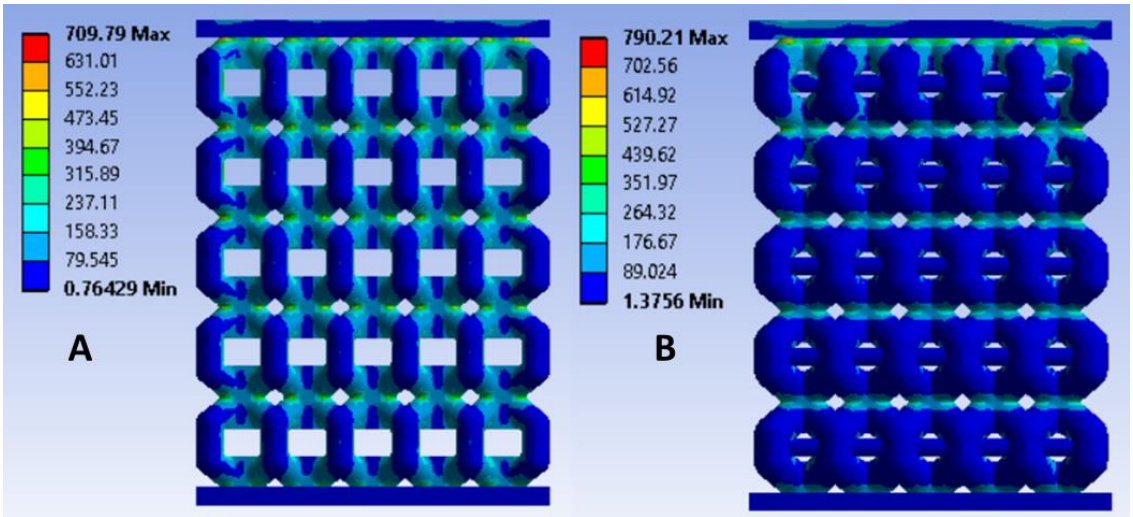

Figure 2.10 Comparison of Stress distribution for 50% porous Design 1 and 30% porous Design 3 structures

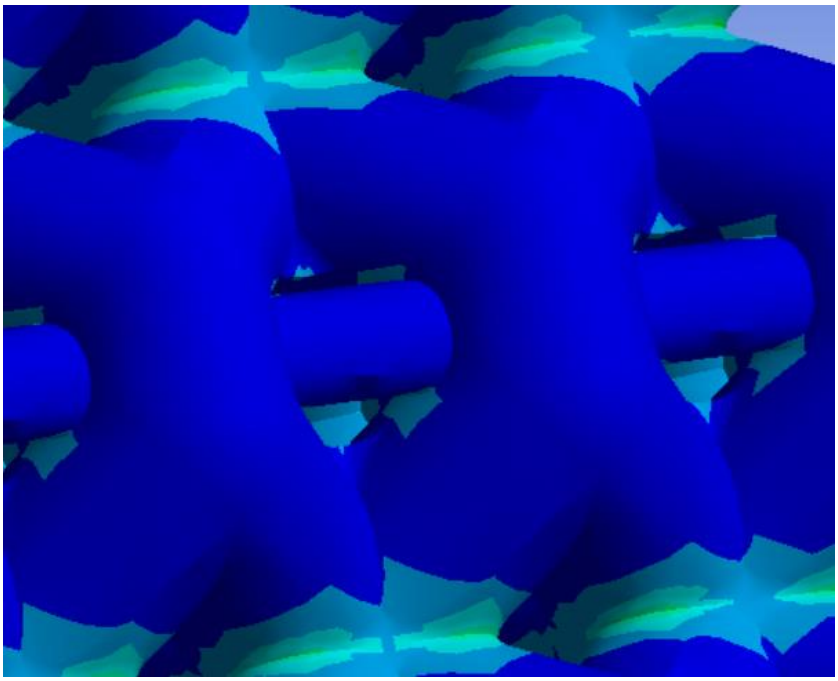

Figure 2.11. Showing Stress concentration regions at intersection of horizontal and vertical members

2.3.2. Structural Characterization

Based on the computational evaluation Design 1 was selected as a suitable material to be printed and tested experimentally (as seen from Table 2.1.). The octahedron

structure was also printed as a validation sample set as it showed similar behaviour to the design 1 structure.

The structures as viewed under an SEM can be seen in Fig. 2.12 and Fig. 2.13. Although the surface is rough and irregular, the structs are continuous and well-formed for the most part. However, some defects that are inherent for structures like these are observed (Fig. 2.15). Missing struts, over melting and broken struts were observed in most structures which contribute to a less than ideal structure. It is crucial to note that the values obtained by experimental testing are conservative values because they do not account for bone growing into implant structure and further reinforcing the structure.

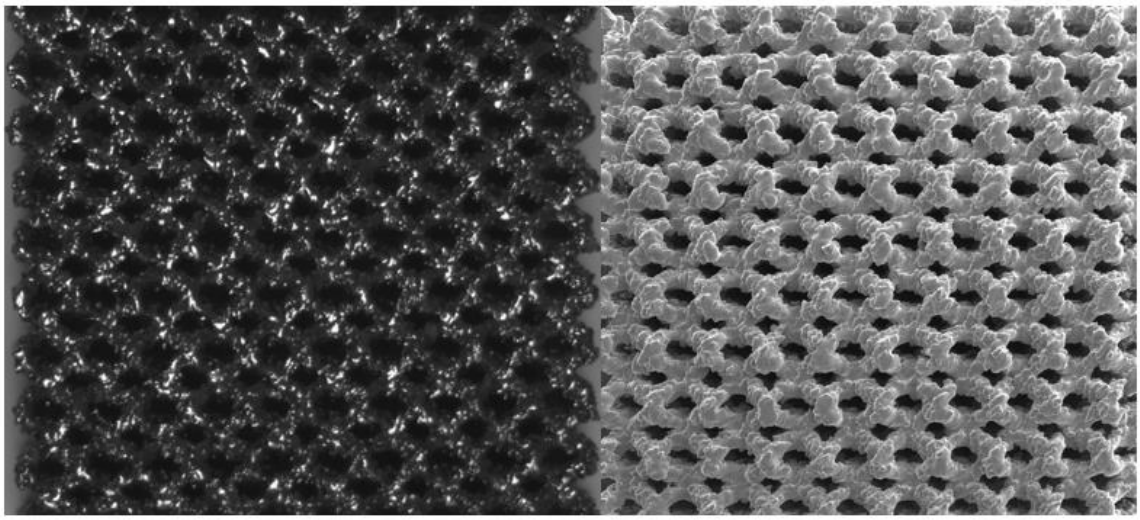

Figure 2.12. Design 1 structure as seen under DIC camera and SEM.

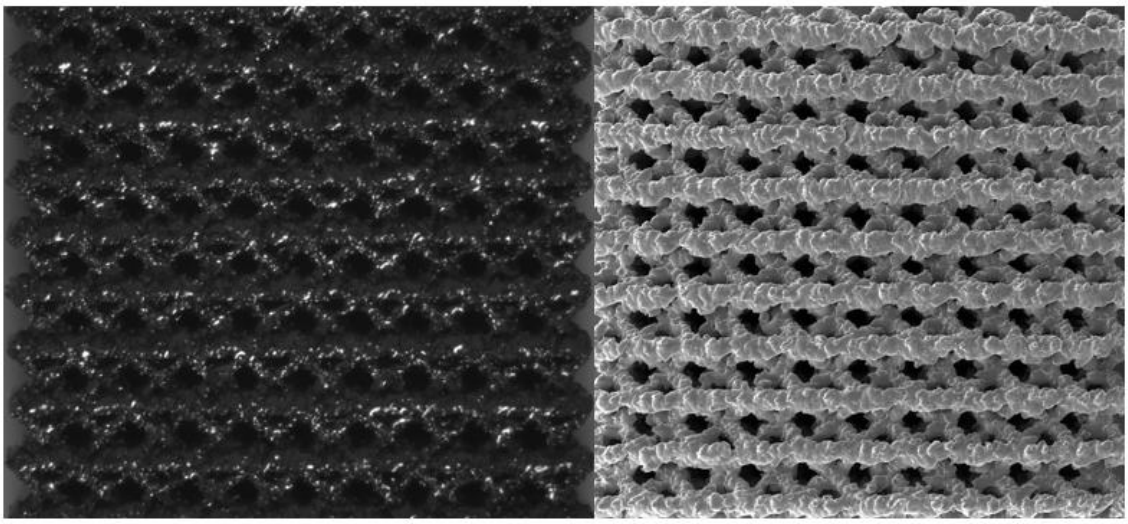

Figure 2.13. Octahedron structure as seen under DIC camera and SEM.

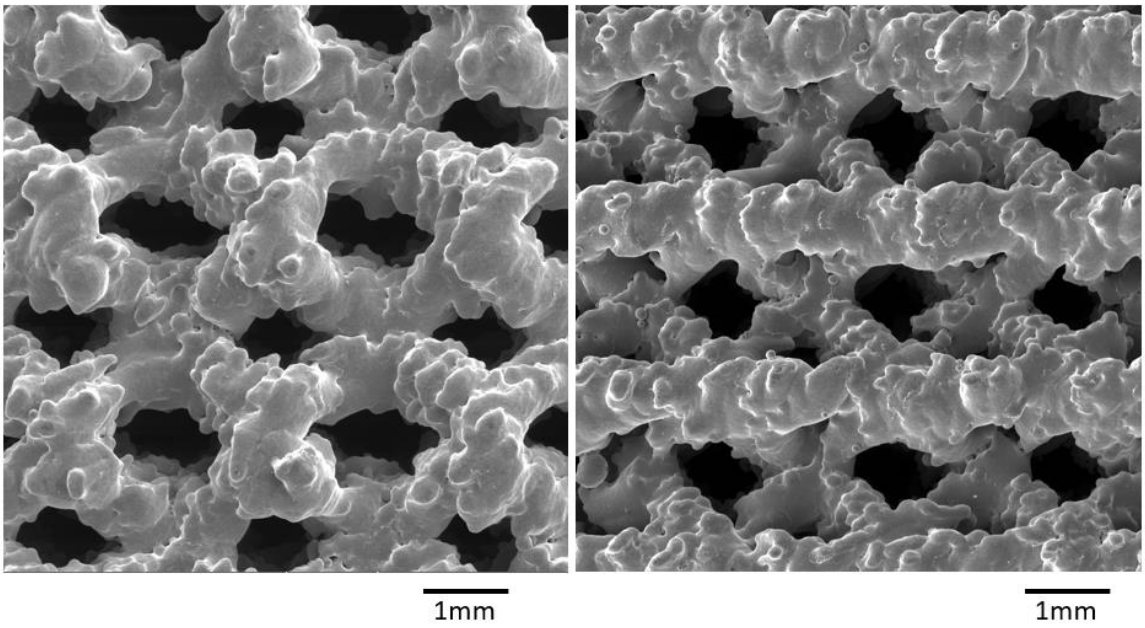

Figure 2.14. The two structures seen at a high magnification. Design 1 is shown on the left and Octahedron is shown on the right.

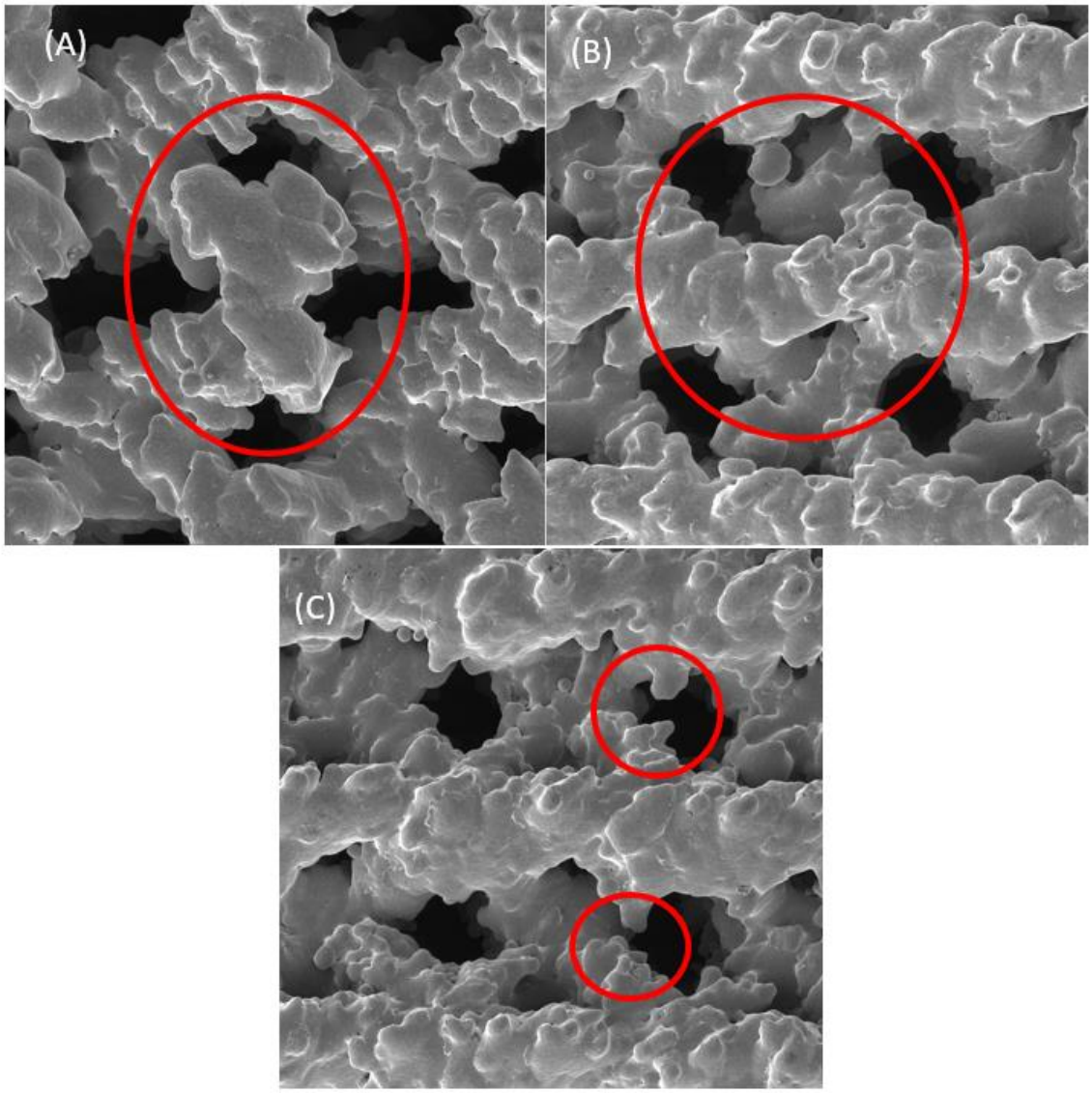

Figure 2.15. Defects as observed under the SEM. (A) Broken Struts. (B) Missing Struts. (C) Over-melting.

2.3.3. Mechanical Behaviour

Fig. 2.16 shows the stress-strain curves for the printed structures. Clear linear regions are observed for both the structures, following which a plastic collapse is observed as depicted by the long plateau region. When struts are pressed together, a sharp rise in the stress-strain curve is seen again. Fig. 2.17. shows the samples before and after

compression. The test was stopped for the octahedron structures when the load limit was reached, at which point the sample was completely compacted with the pores shut. Design 1 structures one the other hand failed with an approximately 45º inclined fracture. Although the Young's modulus was a lot lower than the computational values, they were as close to bone as possible which makes these structures suitable to be used as biomaterials. The elastic modulus of the structures is given in Table 2.3.

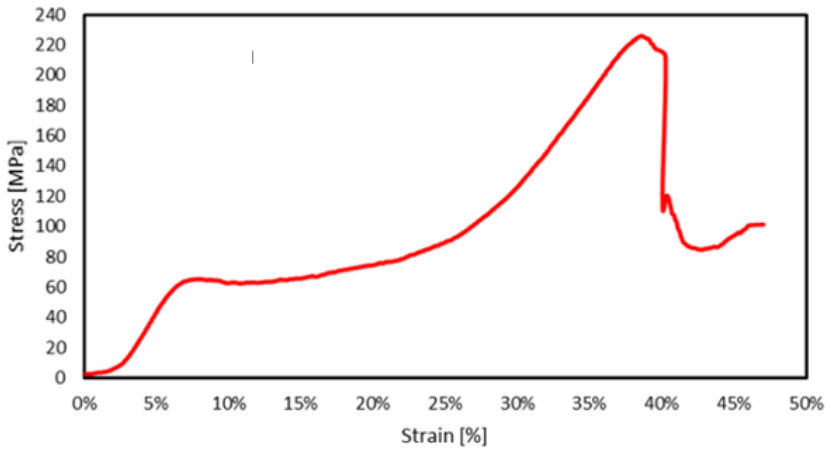

Figure 2.16. a. Stress-Strain Curve for Design 1 (50% Porosity).

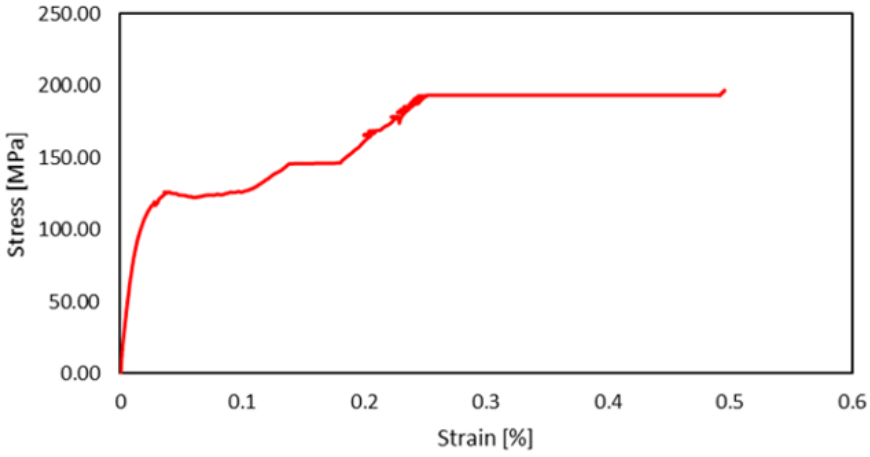

Figure 2.16. b. Stress-Strain Curve for Octahedron (50% Porosity).

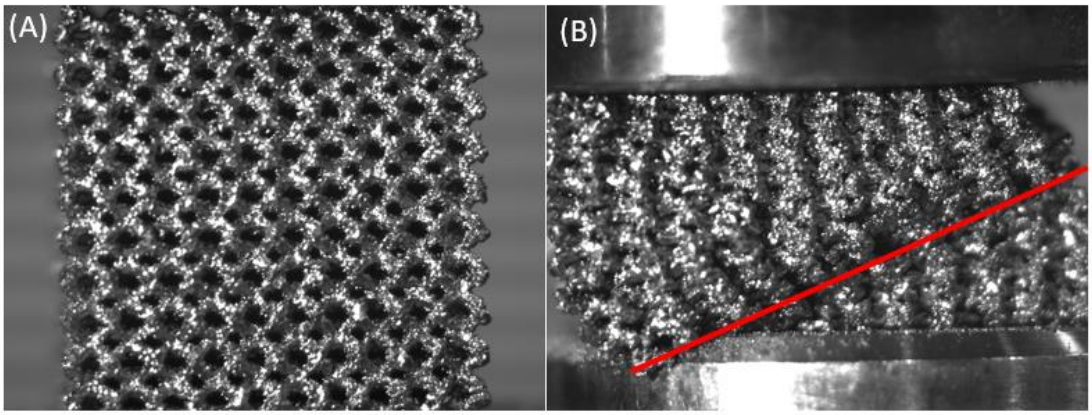

Figure 2.17. a. Design 1 structure before and after compression. (A) Shows the structure before compression. (B) The failed structure after failure.

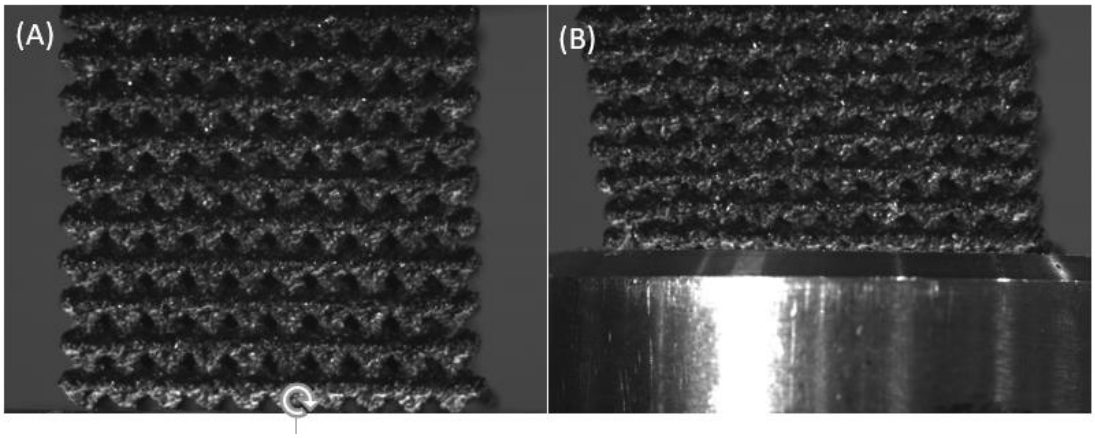

Figure 2.17. b. Octahedron structure before and after compression. (A) Shows the structure before compression. (B) Shows the structure at the end of compression.

Table 2.3: Experimental results for Static Testing of the lattice structures.

Structure	Porosity	Young's Modulus	Yield Stress
Design 1	57%	1.7 ± 0.4 GPa	69.13 ± 13.05 GPa
Octahedron	55%	8.1 ± 0.52 GPa	98.5 ± 4.94 GPa

2.4. Discussion

We systematically designed and studied Ti64 lattice structures manufactured using EBM that showed bone-mimicking properties. Topology optimization was used to design novel structures with the goal of having low elastic modulus yet sufficiently high fatigue life. With the approach demonstrated in this paper computational tools can be used to design and shortlist design structures depending on the field of application. Moreover, the versatility of this method allows the designer to manufacture structures tailor-made for different applications. As shown in this work, we were able to use the same approach to create structures with an elastic modulus as low as 7.5 GPa and structures with a modulus as high as 60 GPa (Table 2.1).

The advantage of this approach to designing materials is that it saves the cost to manufacture and test various structures when one could rather just computationally test a vast number of structures and use rapid prototyping to validate suitable structures. However, it is important to consider that this method incurs a significantly higher computational cost. Furthermore, an increase in research on deep learning [52–54] and neural networks [55,56] promises to improve the efficiency of design tools for creating novel structures using tools like topology optimization.

Using this method, we were able to design porous structures with mechanical properties suitable for fabricating implants. Computationally, we determined which structures were suitable for fabrication. Theoretical Young's modulus as low as 7.5 GPa was achieved which matches that of bone. At the same time these structures showed theoretical fatigue behaviour higher than the benchmark as well. The structures that showed properties suitable to be used as biomaterials were printed sing EBM to evaluate the mechanical properties of the printed structures as it is known that the properties will tend to be lower than the computational counterparts. However, as bone grows into the pores, the overall structure of the implant is strengthened and add to the mechanical integrity of these structures. The fatigue properties of these structures as printed and the change in mechanical behaviour after post processing treatments like hot-isostatic pressing will be the focus of the future work of this study.

CONCLUSION

Topology Optimization and AM was used to design titanium lattice structures with bone-mimicking properties. A systematic approach to this design was shown in this paper. The parameters of these structures such as pore size, porosity and surface treatment have important effect on the growth of bone. If designed correctly these structures can be tuned to behave like superior biomaterials in order to manufacture implants with higher longevity.

REFERENCES

[1] W.E. Frazier, Metal additive manufacturing: A review, J. Mater. Eng. Perform. 23 (2014) 1917–1928. https://doi.org/10.1007/s11665-014-0958-z.

[2] Z. Xiao, Y. Yang, R. Xiao, Y. Bai, C. Song, D. Wang, Evaluation of topology-optimized lattice structures manufactured via selective laser melting, Mater. Des. 143 (2018) 27–37. https://doi.org/10.1016/j.matdes.2018.01.023.

[3] T. Maconachie, M. Leary, B. Lozanovski, X. Zhang, M. Qian, O. Faruque, M. Brandt, SLM lattice structures: Properties, performance, applications and challenges, Mater. Des. 183 (2019) 108137. https://doi.org/10.1016/j.matdes.2019.108137.

[4] P. Regenfuss, A. Streek, L. Hartwig, S. Klötzer, T. Brabant, M. Horn, R. Ebert, H. Exner, Principles of laser micro sintering, Rapid Prototyp. J. 13 (2007) 204–212. https://doi.org/10.1108/13552540710776151.

[5] M. Kadic, G.W. Milton, M. van Hecke, M. Wegener, 3D metamaterials, Nat. Rev. Phys. 1 (2019) 198–210. https://doi.org/10.1038/s42254-018-0018-y.

[6] X. Wu, Y. Su, J. Shi, Perspective of additive manufacturing for metamaterials development, Smart Mater. Struct. 28 (2019). https://doi.org/10.1088/1361-665X/ab2eb6.

[7] X. Yu, J. Zhou, H. Liang, Z. Jiang, L. Wu, Mechanical metamaterials associated with stiffness, rigidity and compressibility: A brief review, Prog. Mater. Sci. 94 (2018) 114–173. https://doi.org/10.1016/j.pmatsci.2017.12.003.

[8] C.P. de Jonge, H.M.A. Kolken, A.A. Zadpoor, Non-auxetic mechanical metamaterials, Materials (Basel). 12 (2019). https://doi.org/10.3390/ma12040635.

[9] X.Z. Zhang, M. Leary, H.P. Tang, T. Song, M. Qian, Selective electron beam manufactured Ti-6Al-4V lattice structures for orthopedic implant applications: Current status and outstanding challenges, Curr. Opin. Solid State Mater. Sci. 22 (2018) 75–99. https://doi.org/10.1016/j.cossms.2018.05.002.

[10] I.M. Raza, L. Iannucci, P.T. Curtis, Additive manufacturing of locally resonant composite metamaterials, ECCM 2016 - Proceeding 17th Eur. Conf. Compos. Mater. (2016).

[11] S. Chen, Y. Fan, Q. Fu, H. Wu, Y. Jin, J. Zheng, F. Zhang, A review of tunable acoustic metamaterials, Appl. Sci. 8 (2018). https://doi.org/10.3390/app8091480.

[12] K.H. Matlack, A. Bauhofer, S. Krödel, A. Palermo, C. Daraio, Composite 3D-printed metastructures for lowfrequency and broadband vibration absorption, Proc. Natl. Acad. Sci. U. S. A. 113 (2016) 8386–8390. https://doi.org/10.1073/pnas.1600171113.

[13] S. Arabnejad, B. Johnston, M. Tanzer, D. Pasini, Fully porous 3D printed titanium femoral stem to reduce stress-shielding following total hip arthroplasty, J. Orthop. Res. 35 (2017) 1774–1783. https://doi.org/10.1002/jor.23445.

[14] H. Kang, J.P. Long, G.D. Urbiel Goldner, S.A. Goldstein, S.J. Hollister, A

paradigm for the development and evaluation of novel implant topologies for bone fixation: Implant design and fabrication, J. Biomech. 45 (2012) 2241–2247. https://doi.org/10.1016/j.jbiomech.2012.06.011.

[15] Y. Yang, G. Wang, H. Liang, C. Gao, S. Peng, L. Shen, C. Shuai, Additive manufacturing of bone scaffolds, Int. J. Bioprinting. 5 (2019) 1–25. https://doi.org/10.18063/IJB.v5i1.148.

[16] H. ZHOU, X. ZHANG, H. ZENG, H. YANG, H. LEI, X. LI, Y. WANG, Lightweight structure of a phase-change thermal controller based on lattice cells manufactured by SLM, Chinese J. Aeronaut. 32 (2019) 1727–1732. https://doi.org/10.1016/j.cja.2018.08.017.

[17] L. Zhang, L. Chen, A Review on Biomedical Titanium Alloys: Recent Progress and Prospect, Adv. Eng. Mater. 21 (2019) 1801215. https://doi.org/10.1002/adem.201801215.

[18] S.J. Macinnes, the Genetics of Osteolysis and Heterotopic Ossification After Total Hip Arthroplasty, (2016).

[19] M. Sundfeldt, L. V. Carlsson, C.B. Johansson, P. Thomsen, C. Gretzer, Aseptic loosening, not only a question of wear: A review of different theories, Acta Orthop. 77 (2006) 177–197. https://doi.org/10.1080/17453670610045902.

[20] R. Huiskes, H. Weinans, B. Van Rietbergen, The relationship between stress shielding and bone resorption around total hip stems and the effects of flexible materials, Clin. Orthop. Relat. Res. (1992) 124–134. https://doi.org/10.1097/00003086-199201000-00014.

[21] C.Y. Lin, N. Kikuchi, S.J. Hollister, A novel method for biomaterial scaffold internal architecture design to match bone elastic properties with desired porosity, J. Biomech. 37 (2004) 623–636. https://doi.org/10.1016/j.jbiomech.2003.09.029.

[22] T. Winkler, F.A. Sass, G.N. Duda, K. Schmidt-Bleek, A review of biomaterials in bone defect healing, remaining shortcomings and future opportunities for bone tissue engineering: The unsolved challenge, Bone Jt. Res. 7 (2018) 232–243. https://doi.org/10.1302/2046-3758.73.BJR-2017-0270.R1.

[23] A. Sutradhar, G.H. Paulino, M.J. Miller, T.H. Nguyen, Topological optimization for designing patient-specific large craniofacial segmental bone replacements, Proc. Natl. Acad. Sci. U. S. A. 107 (2010) 13222–13227. https://doi.org/10.1073/pnas.1001208107.

[24] P. Stoor, A. Suomalainen, C. Lindqvist, K. Mesimäki, D. Danielsson, A. Westermark, R.K. Kontio, Rapid prototyped patient specific implants for reconstruction of orbital wall defects, J. Cranio-Maxillofacial Surg. 42 (2014) 1644–1649. https://doi.org/10.1016/j.jcms.2014.05.006.

[25] C. Celenk, P. Celenk, Bone Density Measurement Using Computed Tomography, Comput. Tomogr. - Clin. Appl. (2012). https://doi.org/10.5772/22884.

[26] V. Bruno, C. Berti, C. Barausse, M. Badino, R. Gasparro, D.R. Ippolito, P. Felice, Clinical Relevance of Bone Density Values from CT Related to Dental Implant Stability: A Retrospective Study, Biomed Res. Int. 2018 (2018).

https://doi.org/10.1155/2018/6758245.

[27] A. Ataee, Y. Li, G. Song, C. Wen, Metal scaffolds processed by electron beam melting for biomedical applications, in: Met. Foam Bone Process. Modif. Charact. Prop., 2017. https://doi.org/10.1016/B978-0-08-101289-5.00003-2.

[28] A. Moridi, A.G. Demir, L. Caprio, A.J. Hart, B. Previtali, B.M. Colosimo, Deformation and failure mechanisms of Ti – 6Al – 4V as built by selective laser melting, Mater. Sci. Eng. A. 768 (2019) 138456. https://doi.org/10.1016/j.msea.2019.138456.

[29] A. Mazzoli, M. Germani, R. Raffaeli, Direct fabrication through electron beam melting technology of custom cranial implants designed in a PHANToM-based haptic environment, Mater. Des. 30 (2009) 3186–3192. https://doi.org/10.1016/j.matdes.2008.11.013.

[30] A.L. Jardini, M.A. Larosa, R.M. Filho, C.A.D.C. Zavaglia, L.F. Bernardes, C.S. Lambert, D.R. Calderoni, P. Kharmandayan, Cranial reconstruction: 3D biomodel and custom-built implant created using additive manufacturing, J. Cranio-Maxillofacial Surg. 42 (2014) 1877–1884. https://doi.org/10.1016/j.jcms.2014.07.006.

[31] M. Cronskär, M. Bäckström, L.E. Rännar, Production of customized hip stem prostheses - A comparison between conventional machining and electron beam melting (EBM), Rapid Prototyp. J. 19 (2013) 365–372. https://doi.org/10.1108/RPJ-07-2011-0067.

[32] L.E. Murr, K.N. Amato, S.J. Li, Y.X. Tian, X.Y. Cheng, S.M. Gaytan, E.

Martinez, P.W. Shindo, F. Medina, R.B. Wicker, Microstructure and mechanical properties of open-cellular biomaterials prototypes for total knee replacement implants fabricated by electron beam melting, J. Mech. Behav. Biomed. Mater. 4 (2011) 1396–1411. https://doi.org/10.1016/j.jmbbm.2011.05.010.

[33] M.K. Kamel, A. Cheng, B. Vaughan, B. Stiles, Sternal Reconstruction Using Customized 3D-Printed Titanium Implants, Ann. Thorac. Surg. (2019). https://doi.org/10.1016/j.athoracsur.2019.09.087.

[34] P. Vogiatzis, S. Chen, X. Wang, T. Li, L. Wang, Topology optimization of multi-material negative Poisson's ratio metamaterials using a reconciled level set method, CAD Comput. Aided Des. 83 (2017) 15–32. https://doi.org/10.1016/j.cad.2016.09.009.

[35] V.J. Challis, J.K. Guest, Level set topology optimization of fluids in Stokes flow, Int. J. Numer. Methods Eng. 79 (2009) 1284–1308. https://doi.org/10.1002/nme.2616.

[36] G.I.N. Rozvany, A critical review of established methods of structural topology optimization, Struct. Multidiscip. Optim. 37 (2009) 217–237. https://doi.org/10.1007/s00158-007-0217-0.

[37] K. Liu, A. Tovar, An efficient 3D topology optimization code written in Matlab, Struct. Multidiscip. Optim. 50 (2014) 1175–1196. https://doi.org/10.1007/s00158-014-1107-x.

[38] K. Lietaert, A. Cutolo, D. Boey, B. Van Hooreweder, Fatigue life of additively

manufactured Ti6Al4V scaffolds under tension-tension, tension-compression and compression-compression fatigue load, Sci. Rep. 8 (2018) 1–9. https://doi.org/10.1038/s41598-018-23414-2.

[39] P. Li, D.H. Warner, A. Fatemi, N. Phan, Critical assessment of the fatigue performance of additively manufactured Ti-6Al-4V and perspective for future research, Int. J. Fatigue. 85 (2016) 130–143. https://doi.org/10.1016/j.ijfatigue.2015.12.003.

[40] A.A. Zadpoor, Mechanics of additively manufactured biomaterials, J. Mech. Behav. Biomed. Mater. 70 (2017) 1–6. https://doi.org/10.1016/j.jmbbm.2017.03.018.

[41] C. Zhang, L. Zhang, L. Liu, L. Lv, L. Gao, N. Liu, X. Wang, J. Ye, Mechanical behavior of a titanium alloy scaffold mimicking trabecular structure, J. Orthop. Surg. Res. 15 (2020) 1–11. https://doi.org/10.1186/s13018-019-1489-y.

[42] M. Abdi, I. Ashcroft, R. Wildman, Topology optimization of geometrically nonlinear structures using an evolutionary optimization method, Eng. Optim. 50 (2018) 1850–1870. https://doi.org/10.1080/0305215X.2017.1418864.

[43] A.M. Torres, A.A. Trikanad, C.A. Aubin, F.M. Lambers, M. Luna, C.M. Rimnac, P. Zavattieri, C.J. Hernandez, Bone-inspired microarchitectures achieve enhanced fatigue life, Proc. Natl. Acad. Sci. 116 (2019) 201905814. https://doi.org/10.1073/pnas.1905814116.

[44] S.M. Ahmadi, S.A. Yavari, R. Wauthle, B. Pouran, J. Schrooten, H. Weinans, A.A. Zadpoor, Additively manufactured open-cell porous biomaterials made

from six different space-filling unit cells: The mechanical and morphological properties, Materials (Basel). 8 (2015) 1871–1896. https://doi.org/10.3390/ma8041871.

[45] G. Rotta, T. Seramak, K. Zasińska, Estimation of Young's Modulus of the Porous Titanium Alloy with the Use of Fem Package, Adv. Mater. Sci. 15 (2015) 29–37. https://doi.org/10.1515/adms-2015-0020.

[46] I. Kutzner, B. Heinlein, F. Graichen, A. Bender, A. Rohlmann, A. Halder, A. Beier, G. Bergmann, Loading of the knee joint during activities of daily living measured in vivo in five subjects, J. Biomech. 43 (2010) 2164–2173. https://doi.org/10.1016/j.jbiomech.2010.03.046.

[47] G. Bergmann, A. Bender, F. Graichen, J. Dymke, A. Rohlmann, A. Trepczynski, M.O. Heller, I. Kutzner, Standardized loads acting in knee implants, PLoS One. 9 (2014). https://doi.org/10.1371/journal.pone.0086035.

[48] M. Benedetti, J. Klarin, F. Johansson, V. Fontanari, V. Luchin, G. Zappini, A. Molinari, Study of the compression behaviour of Ti6Al4V trabecular structures produced by additive laser manufacturing, Materials (Basel). 12 (2019). https://doi.org/10.3390/ma12091471.

[49] J. Parthasarathy, B. Starly, S. Raman, A. Christensen, Mechanical evaluation of porous titanium (Ti6Al4V) structures with electron beam melting (EBM), J. Mech. Behav. Biomed. Mater. 3 (2010) 249–259. https://doi.org/10.1016/j.jmbbm.2009.10.006.

[50] S. Li, S. Zhao, W. Hou, C. Teng, Y.L. Hao, Y. Li, R. Yang, R.D.K. Misra,

Functionally Graded Ti-6Al-4V Meshes with High Strength and Energy Absorption: Functionally Graded Ti-6Al-4V Meshes …, Adv. Eng. Mater. 18 (2015). https://doi.org/10.1002/adem.201500086.

[51] S. Amin Yavari, S.M. Ahmadi, R. Wauthle, B. Pouran, J. Schrooten, H. Weinans, A.A. Zadpoor, Relationship between unit cell type and porosity and the fatigue behavior of selective laser melted meta-biomaterials, J. Mech. Behav. Biomed. Mater. 43 (2015) 91–100. https://doi.org/10.1016/j.jmbbm.2014.12.015.

[52] A. Bidgoli, P. Veloso, Deepcloud the application of a data-driven, generative model in design, Recalibration Imprecision Infidelity - Proc. 38th Annu. Conf. Assoc. Comput. Aided Des. Archit. ACADIA 2018. (2018) 176–185.

[53] Y. Yu, T. Hur, J. Jung, I.G. Jang, Deep learning for determining a near-optimal topological design without any iteration, Struct. Multidiscip. Optim. 59 (2018) 787–799.

[54] H. Sasaki, H. Igarashi, Topology optimization accelerated by deep learning, IEEE Trans. Magn. 55 (2019). https://doi.org/10.1109/TMAG.2019.2901906.

[55] B. Harish, K. Eswara Sai Kumar, B. Srinivasan, Topology optimization using convolutional neural network, Lect. Notes Mech. Eng. (2020) 301–307. https://doi.org/10.1007/978-981-15-5432-2_26.

[56] S. Banga, H. Gehani, S. Bhilare, S.J. Patel, L.B. Kara, 3D topology optimization using convolutional neural networks, ResearchGate. (2018).

CHAPTER THREE

CONCLUSIONS AND FUTURE WORK

This thesis aimed at providing a logical and methodical approach to designing porous structures for orthopedic applications. The goal in mind was to design a structure with a Young's modulus close to that of bone to avoid stress-shielding. However, it is essential to keep in mind the trade-off between elastic modulus and fatigue life. This trade-off is one of the biggest barriers when it comes to designing porous structures. As implants are constantly placed under cyclic loading one must be careful to design for both static and cyclic loading conditions.

We used topology optimization to design unit cells that were ideal for a uniaxial loading condition. Then, the suitable unit cells were converted to CAD models and translated into a structure by repeating this unit cell in a 3-dimensional design space. The next step was to determine which structure was ideal for our application. To do this, we used FEA to predict the mechanical properties of the designed structures computationally. As the results in chapter 2 showed, we were able to successfully design structures that showed favorable properties after computational simulations. We then additively manufactured these structures and experimentally tested the static mechanical properties. These results of these tests were in compliant with the computational results, and we indeed were able to design structures that were suitable biomaterials.

A systematic approach to this design was shown through this method. The parameters of these structures such as pore size, porosity and surface treatment have important

effect on the growth of bone. If designed correctly these structures can be tuned to behave like superior biomaterials to manufacture implants with higher longevity. Using tools like FEA saves us the time of manufacturing every sample and testing experimentally. Instead, we computationally predict the values and eliminate those samples that do not lie in the sample space. Although this saves time and manufacturing cost, there is a small price of computational cost and a good understanding of FEM methods that come along with this approach.

Future goals of this work include performing fatigue experiments to verify the computational fatigue life of the printed structures. The loss of a few months early in the year of 2020 due to the COVID – 19 pandemic delayed my schedule and hindered me from achieving this goal. The next step after this should be to perform post-processing on the printed structures such as Hot Isostatic Pressing that is a method of surface treatment. The goal being to see if such post processing techniques alter the performance of these structures and if these alterations are beneficial or not.